Targeted pectin depletion enhances the potential of high-pressure homogenization to increase the network forming potential of tomato cell wall material

Van Audenhove, J.[*], Bernaerts, T., Putri, N. I., Delbaere, S., Caveye, I., Van Loey, A. M. and Hendrickx, M. E.[**]

Laboratory of Food Technology and Leuven Food Science and Nutrition Research Centre (LFoRCe), Department of Microbial and Molecular Systems (M^2S), KU Leuven, Kasteelpark Arenberg 22, Box 2457, 3001, Leuven, Belgium

[*] corresponding author during submission process

jelle.vanaudenhove@kuleuven.be

+32 16 37 32 11

[**] corresponding author after publication

marceg.hendrickx@kuleuven.be

+32 16 32 15 72

Declaration of interest: none

Journal: Food Hydrocolloids

Abstract

The current study addresses the influence of pectin depletion on the potential of high-pressure homogenization (HPH) to increase the network forming potential of the cell wall material (CWM) from tomato. Therefore, the microstructure, water binding capacity and viscoelastic properties of the alcohol-insoluble residue (AIR) and unextractable fractions (UFs) obtained after different levels and methods of pectin extraction were determined in suspension before and after functionalization by HPH. Before HPH, the AIR and the UFs obtained by solvent-based pectin extraction were all characterized by particles displaying cell-like morphology and the storage modulus (G') of the respective suspensions was maximal at partial pectin depletion. The network forming potential of the CWM could only be increased by HPH when extensive disruption of the cell wall network was realized instead of mainly breakage. Even when higher pressure levels were applied (up to 80 MPa), preceding weakening of the cell wall network by pectin extraction was a prerequisite to favor efficient disruption of the CWM during HPH above deformation and breakage. Apart from the effect of partial pectin depletion as such on the cell wall strength, the impact of the extraction conditions (e.g., acid conditions at high temperature) weakening the residual cell wall seems important. This had repercussions on the potential of HPH to functionalize the CWM. While the G' decreased upon HPH (evaluated at 20 MPa) for non-pectin-depleted or partially pectin-depleted CWM generated by using mild extraction conditions, a clear increase was observed upon HPH of CWM which was partially or extensively pectin-depleted using harsher extraction conditions.

Keywords

Tomato

High-pressure homogenization

Pectin extraction

Cell wall material

Rheology

Water binding capacity

Abbreviations and symbols

AcUF: acid-unextractable fraction

AcUF-HPH-AcUF: acid unextractable fraction of the high-pressure homogenized acid-unextractable fraction

AIR: alcohol-insoluble residue

CDTA: cyclohexane-trans-1,2-diaminetetraacetic acid

CUF: chelator-unextractable fraction

CWM: cell wall material

HPH: high-pressure homogenization

lAUF: low-alkaline-unextractable fraction

PSD: volume-based particle size distribution

UF: unextractable fraction

WBC: water binding capacity

$d_{4,3}$: average volume-based particle size

$d_{0.1}$: upper limit of the 10% smallest particles

$d_{0.9}$: upper limit of the 90% smallest particles

G': storage modulus

G": loss modulus

1 Introduction

The plant cell wall is a complex network of polysaccharides, which (generally) assures cell-cell adhesion and gives strength to the plant to resist external forces. However, the cell wall requires, depending on the development stage and/or function of the tissue in the plant, to possess a certain flexibility and porosity (Burton et al., 2010). The cell wall is a supramolecular assembly of pectin, hemicellulose, cellulose and structural proteins (Carpita & Gibeaut, 1993; Jarvis, 2011). In the middle lamella, pectin, which is the main constituent of this layer of the plant cell wall, is responsible for cell-cell adhesion (Daher & Braybrook, 2015). In the primary cell wall, pectin is not only present as a matrix surrounding this network but

effectively interacts with the cellulose-hemicellulose network especially by its neutral side-chains (Cosgrove, 2001, 2014; Zykwinska et al., 2007; Zykwinska, Ralet, Garnier, & Thibault, 2005).

In the context of the quality of plant-based foods, the study of the cell wall properties is also very relevant from a food-technological point of view (Doblin et al., 2010). Indeed, the characteristics of the cell wall have an important repercussion on the textural properties of fruit- and vegetable-based food products (Waldron, Parker, & Smith, 2003). Next to the composition and viscosity of the serum phase, the main factors affecting the rheological properties of fruit and vegetable dispersions are the concentration of the particles, their properties (e.g., size, size distribution, morphology, deformability) and the interactions between the particles (Appelqvist et al., 2015; Moelants, Cardinaels, Van Buggenhout, et al., 2014). In this context, it is of high interest to understand how the network forming potential of this cell wall material (CWM) could be altered and, if possible, optimized by targeted functionalization (Foster, 2011). Foster (2011) suggested four distinct routes of functionalization, namely, the use of enzymes, applying mechanical processing, heating or chemical treatments, or combinations thereof. High-pressure homogenization (HPH) represents a mechanical treatment which is applied in food industry to food systems in the dispersed state aiming to obtain a reduced particle size and/or a good mixing of the ingredients (Levy et al., 2020). The disruptive effect of this treatment, mainly originating from the shear forces on the microstructure of the suspension when the food product is passing through the small valve opening, can alter its rheological properties (Bayod et al., 2007; Bengtsson & Tornberg, 2011; Kubo et al., 2013; Levy et al., 2020; Lopez-Sanchez, Nijsse, et al., 2011). However, the precise effect of HPH depends on the cell wall composition and structure as it affects the resistance to the applied force (Kaur et al., 2021; Levy et al., 2020). Recently, it was shown that suspensions prepared with CWM of citrus peel (Willemsen et al., 2017) and pumpkin pomace (Atencio et al., 2021) had a higher storage modulus (G') when the pectin fraction was partially removed from the CWM by extraction. This was attributed to the voids in the CWM created by the pectin extraction and the resulting higher potential to swell. Furthermore, the G' of the suspension of the CWM fractions of both origins could even be further increased by HPH. In this regard, the removal of pectin seemed to facilitate further expansion of interfibrillar spaces during HPH resulting in an increasing ability to form a network in suspension and in more swelling of the material (Atencio et al., 2021; Sankaran et al., 2015; Willemsen et al., 2017). However, the botanical origin had, even after partial pectin depletion of the fruit and vegetable CWM, a major effect on the outcome of the network forming potential after HPH due to the differences in composition and microstructural attributes (Van Audenhove, Bernaerts, Putri, et al., 2021).

In the current study, tomato is used as a study material, not only because tomato is globally one of the most consumed vegetable crops (both raw and as component in processed products) (Del Valle et al., 2006; Lu et al., 2019), but especially since research on whole tomato tissue (Augusto et al., 2013a, 2013b; Bayod et al., 2007; Bayod & Tornberg, 2011; Lopez-Sanchez, Nijsse, et al., 2011; Tan & Kerr, 2015) and tomato CWM (Redgwell et al., 2008) in dispersed state has shown that the storage modulus (G') of these suspensions could generally be increased by HPH at pressure levels below 50 to 60 MPa by disruption of the tomato cell walls towards fragments of cell walls, fiber particles and released polymers, which have the potential to swell. The main objective of the current study is to gain insight into how preceding pectin depletion could enhance the functionalization of the CWM by HPH (i.e., facilitating the formation of a microstructure which has an increased ability to form a network in suspension). To address the research objective, suspensions of CWM fractions in water were prepared, of which the microstructure, the water binding capacity (WBC) and relevant viscoelastic properties were analyzed. First, non-pectin-depleted CWM and partially pectin-depleted CWM, obtained as the alcohol-insoluble residue (AIR) and the unextractable fraction (UF) after acid extraction respectively, were high-pressure homogenized at different pressure levels (ranging from 10 to 80 MPa) to understand the role of preceding pectin depletion of CWM by acid extraction in enhancing the functionalization of the CWM by HPH by facilitating the disruption. Indeed, it can be hypothesized that the extraction of pectin could reduce the cell wall strength, and as a consequence allow a more efficient disruption of the cell wall network. Secondly, it was evaluated whether HPH (at 20 MPa) could functionalize CWM fractions obtained as the UF after different pectin extraction approaches. On the one hand, stepwise pectin extraction was performed using hot water, a chelating agent and a low-alkaline medium. On the other hand, pectin was extracted by single-step nitric acid extraction (pH 1.6 and 80 °C) and followed by water and acid extraction facilitated by HPH. Indeed, apart from the effect of the residual pectin content on the cell wall strength, the harsher extraction conditions applied (e.g., during acid extraction and low-alkaline extraction) could also additionally affect the cell wall network by their effect on the chemical structure of the residual pectin. Furthermore, by covering the dual role of HPH on the UF after acid extraction, namely to facilitate further pectin extraction and to functionalize the CWM fraction, more insight was gained into the effect of pectin content on the WBC and rheological properties of, specifically, high-pressure homogenized CWM suspensions.

2 Materials and methods

2.1 Generation of cell wall material fractions

San Marzano tomato (*Solanum lycopersicum*) was used as study material in the current work. Na_2CO_3 and HCl were obtained from VWR (Leuven, Belgium) and Fisher Scientific (Merelbeke, Belgium), respectively. Unless mentioned otherwise, all chemicals used were of analytical grade.

The AIR of blanched San Marzano tomato and the different pectin-depleted CWM fractions as generated and characterized by Van Audenhove, Bernaerts, De Smet, et al. (2021) were used. A schematic overview of the extractions performed to generate the UFs is shown in **Supplementary Figure 1** (Van Audenhove, Bernaerts, De Smet, et al., 2021). Briefly, on the one hand, a stepwise extraction of pectin was performed on the AIR. After extraction of pectin with hot water and cyclohexane-trans-1,2-diaminetetraacetic acid (CDTA), as chelating agent, the chelator UF (CUF) was obtained. After extraction of pectin from the CUF using a low-alkaline medium (0.05 M Na_2CO_3), the low-alkaline UF (lAUF) was obtained. On the other hand, a one-step nitric acid extraction (pH 1.6 and 80 °C) was performed on the AIR, resulting in the acid UF (AcUF). To facilitate further pectin extraction, this AcUF was subjected to HPH, followed by extraction with water and with nitric acid under the same conditions as during the first step. After this repeated acid extraction, the AcUF of high-pressure homogenized AcUF was obtained (AcUF-HPH-AcUF). The UFs were frozen with liquid nitrogen and stored at -40 °C until further use. A summary of the most relevant compositional properties in the context of the current study is given in **Table 1** expressed in mol% to the total amount of monosaccharides measured (Van Audenhove, Bernaerts, De Smet, et al., 2021). From this table, it is clear that the UF had different levels of residual pectin content depending on the extraction condition used. The starting material AIR represents CWM (together with a small amount of co-precipitated polymers) without pectin depletion, the CUF and AcUF represent partially pectin-depleted CWM, and the lAUF and AcUF-HPH-AcUF represent extensively pectin-depleted CWM.

Table 1: Contribution of the pectin backbone and contribution of hemicellulose and cellulose ± standard deviation based on the monosaccharide composition (n=2·2). UA = uronic acid; Rha = rhamnose; Glc = glucose; Xyl = xylose; Man = mannose. Data are from Van Audenhove, Bernaerts, De Smet, et al. (2021).

	Contribution of the pectin backbone [mol%] UA + Rha	Contribution of hemicellulose and cellulose [mol%] Glc + Xyl + Man
AIR	39.0 ± 2.2	56.4 ± 2.6

CUF	22.7 ± 1.9	72.7 ± 5.4
lAUF	6.1 ± 0.4	89.2 ± 3.3
AcUF	23.3 ± 1.1	73.9 ± 3.9
AcUF-HPH-AcUF	10.3 ± 0.5	87.3 ± 5.3

160

161 2.2 Preparation of cell wall material suspensions and high-pressure homogenization

162 The dry matter content determination and the suspension preparation were performed according to Van
163 Audenhove, Bernaerts, Putri, et al. (2021). In the case of the AIR, which was in dry state, deionized water
164 was added to reach the desired concentration and the pH was adjusted to pH 4.5 with 1 M HCl. For all the
165 UFs, the CWM was used in wet state, of which the dry matter content was known. After thawing,
166 deionized water was added to obtain suspensions with the desired concentration. The pH was adjusted
167 to pH 4.5 using 2 M Na_2CO_3 for the AcUF and AcUF-HPH-AcUF and 1 M HCl for the CUF and lAUF. A 1%
168 (w/w) suspension was prepared from the AIR and AcUF. The suspension was stored overnight at room
169 temperature to assure complete hydration. Then, the suspension was mixed for 10 min at 8000 rpm (Ultra
170 Turrax T25, IKA, Staufen, Germany). This suspension was divided in aliquots, which were non-high-
171 pressure homogenized or high-pressure homogenized at one of the pressure levels studied (i.e., 10, 20,
172 40, 60 and 80 MPa) (Panda 2k, GEA Niro Soavi, Parma, Italy). Furthermore, a 2% (w/w) suspension was
173 prepared from the AIR and each of the UFs. The suspension was stored overnight and mixed for 10 min at
174 8000 rpm (Ultra Turrax T25, IKA, Staufen, Germany). Part of the suspension was not high-pressure
175 homogenized (0 MPa) and the other part was high-pressure homogenized at 20 MPa. The suspension
176 preparation was performed in duplicate.

177 2.3 Characterization of the microstructural and functional properties of the cell wall
178 material in suspension

179 The microscopic, particle size, rheological and water binding capacity analyses were performed exactly as
180 described by Van Audenhove, Bernaerts, Putri, et al. (2021).

181 2.3.1 Microscopic analysis

182 Light microscopy in differential interference contrast mode at magnification 10x (Olympus BX-51,
183 Olympus Optical Co. Ltd., Tokyo, Japan) was used to visualize the microstructure of the suspension (100
184 µL; 0.6% w/w). The pictures were taken with a XC-50 digital camera. A representative micrograph was
185 chosen out of around ten images.

2.3.2 Particle size distribution analysis

Laser diffraction analysis (Laser Diffraction Particle Size Analyzer, LS 13 320, Beckman Coulter Inc., Indianapolis, IN, USA) was performed to determine the volume-based particle size distribution (PSD) ranging from 0.04 to 2000 µm using the Fraunhofer model. The average volume-based particle size ($d_{4,3}$) and, if relevant, also the $d_{0.1}$ and $d_{0.9}$ were calculated, which are the upper limits of the 10% and 90% smallest particles, respectively. The measurement (consisting of two consecutive runs of 90 s) was performed at pump speed 30% and at obscuration around 8-10% (diluted in deionized water). Only the data of the second run was used for the calculations. The analysis was performed in duplicate.

2.3.3 Rheological analysis

The rheological analysis was performed at 25 °C with a stress controlled rheometer (MCR 302, Anton Paar, Graz, Austria) and a concentric cylinder system (2 mm gap) with rough surfaces designed by Willemsen et al. (2018). After the sample was loaded in the cup, the following sequence of steps was executed: a pre-shear (1 min at 10 s^{-1}), a rest period of 1 min, a time sweep (3 min, angular frequency 10 rad/s and strain 0.1%), a frequency sweep (angular frequency logarithmically decreasing from 100 rad/s to 0.1 rad/s and strain 0.1%), a second time sweep (1 min, angular frequency 10 rad/s and strain 0.1%) and a strain sweep (angular frequency of 10 rad/s and logarithmically increasing strain from 0.01% to 100%). The analysis was done in duplicate (loaded twice).

2.3.4 Measurement of water binding capacity

Centrifugation at 1000g for 30 min at 25 °C (LUMiFuge, LUM GmbH, Berlin, Germany) was performed on the suspensions (1% w/w or 2% w/w) of the AIR and the UFs to evaluate their WBC, which was calculated using eq. 1.

$$\mathrm{WBC} = \frac{\text{mass suspension}\cdot x - \text{mass of supernatant}}{\text{mass suspension}\cdot(1-x)} \qquad \text{[eq. 1]}$$

where WBC is the water binding capacity [g water/g], x is a constant which is 0.99 and 0.98 for the 1% and 2% (w/w) suspension, respectively.

The analysis was performed in duplicate as two cuvettes were filled for each suspension.

2.4 Statistical analysis

All suspensions were prepared twice, on each suspension all analyses were performed in duplicate (i.e., n=2·2). The average and standard deviation were calculated on these four values. The Tukey's range test

was performed to test for significant differences between means ($P < 0.05$) (JMP Pro 15, SAS Institute Inc., Cary, NC, USA).

3 Results and discussion

3.1 The effect of pressure level during HPH on the microstructural properties of non- and partially pectin-depleted cell wall material

The general microstructural attributes of the AIR and AcUF suspensions obtained by HPH at different pressure levels are visualized in the micrographs in **Figure 1.** Before HPH, the particles in both the AIR and AcUF suspensions still showed cell-like morphology and seemed to occur separately. One could describe it as single cells as is done in literature on fruit and vegetable dispersions in which the cells are occurring separately (not in clusters or intact tissue) (Appelqvist et al., 2015; Day et al., 2010; Lopez-Sanchez et al., 2012), however, it should be stipulated that mainly only the CWM, although its composition possibly affected by the extraction conditions, is still present in the current study. This (almost) complete cell separation during the high intensity mixing applied while preparing the AIR from the tissue was probably promoted by the (partial) solubilization of the pectin in the middle lamella responsible for cell-cell adhesion during ripening of the tomato and during the high-temperature blanching (Daher & Braybrook, 2015; Waldron, Smith, Parr, Ng, & Parker, 1997). The PSDs of the particles in the AIR and AcUF before HPH were different (**Figure 2**). While a $d_{4,3}$ of 494 ± 10 µm and a tail towards larger particle sizes (above 1000 µm) was observed in the PSD of the AIR suspension, a $d_{4,3}$ of 370 ± 2 µm and a PSD without tailing to larger sizes was obtained for the AcUF. The $d_{4,3}$ of the AcUF is in line with the size of single tomato cells determined by other authors (Becker et al., 1972; Lopez-Sanchez et al., 2012). Based on the broad range observed between the $d_{0.1}$ and the $d_{0.9}$, respectively 158 ± 1 µm and 589 ± 4 µm, it is clear that a high variation in cell size existed as was also visible in the micrographs. In the case of the AcUF, it is evident that the ability of the middle lamella to keep the cells together was completely lost, due to the partial extraction of pectin while preparing the AcUF (Daher & Braybrook, 2015). This rationalizes that the large particles present in the AIR, which represent small cell clusters (two or few cells which were still connected) (Lopez-Sanchez, Svelander, et al., 2011), were absent in the AcUF. Nevertheless, based on the PSD and the $d_{0.9}$ which was 847 ± 27 µm, it is clear that even in the AIR suspension the contribution of the large particles to the total was rather limited.

As could be expected (Bayod et al., 2007, 2008; Bayod & Tornberg, 2011; Kubo et al., 2013; Lopez-Sanchez, Nijsse, et al., 2011; Tan & Kerr, 2015), the extent of breakage and/or disruption was higher when higher

pressure levels were applied, which was reflected by the stepwise decrease in $d_{4,3}$ when evaluating higher pressure levels (up to 80 MPa). However, the decrease in particle intactness (**Figure 1**) and size (**Figure 2**) with increase in pressure level was more prominent for the AcUF than for the AIR. At low pressure levels (10 and 20 MPa), the cell walls of the AIR were only slightly deformed or broken locally. This visual observation is confirmed by the particle size data showing no shift of the peak of the PSD to smaller sizes upon HPH at low pressure level. At these pressure levels, the effect of HPH on the AIR was mainly limited to the breakdown of the particles with large dimensions (> 1000 µm) and the generation of a small amount of cell wall fragments (in the range of 50 – 250 µm). These two effects, which occurred to a larger extent at 20 than at 10 MPa, resulted in a small decrease in the $d_{4,3}$ to 443 ± 13 µm and to 406 ± 12 µm after HPH at 10 and 20 MPa, respectively. From 40 MPa onwards, also the peak of the PSD shifted to smaller sizes (**Figure 2A**) and an overall breakdown of the cell-like particles was observed (**Figure 1**). A clear decrease in the particle size of the AcUF by HPH was already observed at 10 MPa. The higher susceptibility of the AcUF to breakdown compared to the AIR can be attributed to the reduced cell wall strength due to the partial pectin extraction. With increasing the pressure level, the peak of the PSD slightly shifted further to lower particle sizes and the fraction of particles having the original dimensions, which was very small in amount even after HPH at 10 MPa, disappeared.

Interestingly, the microstructure of the AIR and AcUF suspensions after impact by HPH was visually different. Whereas cell wall structures were still visible in the case of the AIR for all pressure levels applied, the microstructure of the AcUF could best be described as a continuum of cell wall remnants and fragments without clear cell wall structures. Thus, the partial pectin depletion of the cell wall by the acid extraction led to a different impact of HPH on the CWM microstructure. In fact, in the case of the AIR, the impact of HPH was limited to breakage of the cell-like particles. On the other hand, HPH on the AcUF resulted not only in breakage, but also in disruption of the interactions between the cell wall polymers. Due to the lower strength of the cell wall by the partial pectin depletion obtained by acid extraction, the force needed to overcome the interfibrillar interactions in the cell wall network could be reached by HPH, as was also observed by Willemsen et al. (2017) for AcUF of lemon peel. This extensive disruption already occurred from 10 MPa. Further increasing the pressure level had only a limited effect of the size of the fragments obtained. Although a higher pressure during HPH could be needed depending on the matrix studied, a comparable effect of HPH on the microstructure was also observed for the AcUF of apple, carrot, onion and pumpkin (Van Audenhove, Bernaerts, Putri, et al., 2021).

3.2 The effect of pressure level during high-pressure homogenization on the functional properties of non- and partially pectin-depleted cell wall material in suspension

3.2.1 Water binding capacity

It must be noted that a high amount (around 80-92%) of water in plants is present as intracellular water (Khan et al., 2016), however, in the systems of the current study only the cell walls of the cells were still present. Nevertheless, the water which could stay entrapped by the cells was expected to have a relevant contribution to the WBC (Van Audenhove, Bernaerts, Putri, et al., 2021). Since centrifugation could affect the physical structure of the fibers, it should be noted that comparing the WBC obtained by different researchers is challenging given the variation in methods used for the determination of the hydration properties of fibers (Auffret et al., 1994). Therefore, the intensity of the applied centrifugal force is an important factor in interpreting results on the WBC determination. However, since the centrifugal force for the determination of the WBC used in the current study was lower (1000g for 30 min) than during preparation of the UFs (8000g for 10 min), which did not result in a visual effect on the cell morphology (**Figure 1**, 0 MPa), it is assured that the structural space formed by the intact (pectin-depleted) cell walls in which water can stay enclosed was retained during centrifugation. Important ways of water binding on insoluble polysaccharides are hydrogen bonds, ionic bonds and hydrophobic interactions (Chaplin, 2003; Thebaudin et al., 1997). Moreover, given that the cell wall is a porous network of polymers (Carpita & Gibeaut, 1993; Carpita, Sabularse, Montezinos, & Delmer, 1979), an additional amount of water can be held in pores or capillaries by surface tension strength (López et al., 1996; Thebaudin et al., 1997; Ulbrich & Flöter, 2014). In this context, Willemsen et al. (2017) suggested that water could penetrate into the voids created in the CWM by pectin extraction. This effect of the pectin extraction could rationalize why the WBC (at 1% w/w) of the AIR was lower than for the AcUF (**Figure 3**).

While HPH resulted in a limited decrease in the WBC of the AIR (not significant after HPH at 20 and 40 MPa), an increase was observed for the AcUF. The pressure level used during HPH, on the other hand, had only a very limited effect on the WBC. Van Buggenhout et al. (2015) observed for orange pulp fiber suspensions that smaller particles could bind more water in suspension and display a higher WBC, because of their larger specific surface. However, based on the results, it is clear that the particle size of the CWM was not the only factor determining the WBC. If so, the WBC would increase both for the AIR and AcUF and further increase with the increase in pressure level applied. Since especially the shear-induced exposure of a higher amount of polar groups on this larger surface to the serum phase results in an increased interaction with water (McCann et al., 2011; Van Buggenhout et al., 2015), the opposite effect

observed for the AIR and AcUF is very reasonable taking into account the different impact of HPH on their cell wall network. Indeed, without preceding partial pectin depletion and thus without weakening of the cell wall (as is the case for the AIR), the cell-like morphology was lost mainly due to breakage of which the extent was depending on the pressure level applied. As a consequence, the water being enclosed by the cell walls was lost (even by the limited breakage observed at 10 MPa) and not compensated by an increase in water binding sites by HPH. In contrast, facilitated by the preceding partial pectin depletion of the cell wall network by acid extraction, HPH could rupture the cell wall network of the AcUF, which likely led to a more accessible CWM network having more voids which allows swelling of the material (Atencio et al., 2021; Sankaran et al., 2015; Willemsen et al., 2017) and to more material being exposed to the serum phase than what was possible for the AIR.

3.2.2 Viscoelastic properties

The viscoelastic properties of the AIR and AcUF suspensions before and after HPH at different pressure levels were determined at 1% (w/w). It was observed that the critical strain, which is defined here as the strain resulting in a decrease in G' to 90% of the G' at low strain (Van Audenhove, Bernaerts, Putri, et al., 2021), of all suspensions analyzed was higher than 0.1% (**Figure 4**), assuring that the characterization of the rheological properties by the performed frequency sweep at 0.1% strain is legitimate, since measurements performed within the linear viscoelastic region are not expected to induce irreversible structural changes to the sample (Steffe, 1996). In **Supplementary Figure 2**, the relation between the angular frequency [rad/s] and the G' and G" [Pa] is shown for each suspension. These relations are comparable to what was observed for other fruit- and vegetable-based suspensions (Day et al., 2010; Gundurao et al., 2011; Kotcharian et al., 2004; Kunzek et al., 1999; Müller & Kunzek, 1998; Redgwell et al., 2008; Van Audenhove, Bernaerts, Putri, et al., 2021; Vetter & Kunzek, 2003a, 2003b; Wang et al., 2018). Firstly, the ratio of G"/G' [-], evaluated at 10 rad/s, was below 0.2 for all AIR and AcUF suspensions measured, indicating the existence of a gel-like elastic network (Steffe, 1996). Secondly, based on the low dependency of the G' on the angular frequency (**Supplementary Figure 2**), the suspensions could be classified as "physical gels" (Bayod et al., 2008; Kavanagh & Ross-Murphy, 1998; Rao, 2014). This type of gel is intermediate between "true gels" formed by covalently cross-linked matter, of which the G' is (almost) independent of the frequency, and networks originating from entanglements rather than by cross-links, of which the G' is greatly dependent on the frequency (Bayod et al., 2008; Kavanagh & Ross-Murphy, 1998; Rao, 2014). Thirdly, taking into account the low critical strain, the gels can be classified as being rather weak physical gels (Kavanagh & Ross-Murphy, 1998). In practice, the differences in the relation of the G' with angular frequency among the suspensions studied was mainly limited to lower or

higher absolute values of the G' and G", with the dependency of the G' and G" of the angular frequency being rather similar for all suspensions. Therefore, the G' at a fixed angular frequency (10 rad/s) and strain (0.1%) (**Figure 5**) and the critical strain at a fixed angular frequency (10 rad/s) (**Figure 4**) are further compared as a measure for the stiffness and strength of the suspension, respectively (Moelants, Cardinaels, Jolie, et al., 2014; Willemsen et al., 2017).

As the particles still had cell-like morphology before HPH, the network was formed by packing of these particles (Leverrier et al., 2021; Lopez-Sanchez et al., 2012). The G' of the non-high pressure homogenized AIR and AcUF suspensions was 78 ± 12 and 262 ± 10 Pa, respectively. Interestingly, the partial pectin depletion by acid extraction thus resulted in a clear increase in the G'. This difference between the network forming potential of non-pectin-depleted and (partially) pectin-depleted CWM was also observed by Atencio et al. (2021) and Willemsen et al. (2017) for pumpkin pomace and lemon peel, respectively.

The critical strain of the AIR and AcUF suspensions significantly increased by HPH (**Figure 4**). This was in accordance to the observation of Lopez-Sanchez & Farr (2012) that the critical strain of fragments of tomato cells was higher than of individual cells and cell clusters. This was attributed on the one hand to the increased surface which can lead to more interaction points between particles, and on the other hand to a higher possibility to form (polymer) entanglements (Lopez-Sanchez & Farr, 2012). Hydrogen bonding, van der Waals forces, hydrophobic interactions and electrostatic interactions are the main interactions expected to occur between the cell wall polymers in these suspensions (Kavanagh & Ross-Murphy, 1998; Rao, 2014). In the case of the AIR suspension, the critical strain gradually increased with increasing the pressure level during HPH, or equivalently, with increasing the extent of breakage. On the other hand, a prominent increase in the critical strain of the AcUF suspension was already observed after HPH at 10 MPa in line with the high impact of this treatment on the microstructure. More extensive disruption of the material, obtained by using higher pressure levels, only led to small further increase in the critical strain.

While the network in the AIR suspension was constituted of large particles before HPH, HPH mainly resulted in a breakdown of the cell-like particles to a clearly increasing extent with increasing pressure level. It was also observed in other fruit- and vegetable-based systems that the network forming potential of fragments of cells is lower than for intact cells (Appelqvist et al., 2015; Leverrier et al., 2016). The decreasing ability to form this packed particle network due to the gradual breakdown of the cell-like particles over the pressure levels studied is reflected by the gradual decrease in G'. Since the original morphology was still well retained after HPH at the lowest pressure levels (10 and 20 MPa), the impact of these treatments on the G' of the AIR suspension was still negligible.

Interestingly, although also HPH of the AcUF suspension resulted in particle size reduction, which was even much more prominent than what was the case for the AIR suspension, the G' of the AcUF suspension highly increased by HPH with an optimum at 10 to 20 MPa (**Figure 5**). This dissimilarity between the effect of HPH on the AIR and AcUF highlights that the acid pectin extraction enhanced the potential of HPH to functionalize the CWM. While HPH (especially from 40 MPa onwards) on the AIR was mainly limited to a breakage of the structural entities resulting in fragments with low ability to form a stiff network, the weakening of the cell wall by this pectin extraction facilitated the disruption of the cell wall network instead of mainly only breakage. This efficient disruption likely facilitated the formation of more and/or other interactions between the cell wall polymers as a consequence of the more accessible nature of the cell wall network after HPH. Moreover, this disrupted CWM also possesses a higher potential to swell as was also suggested by Lopez-Sanchez, Nijsse, et al. (2011) for tomato and reflected in the higher WBC of the AcUF after HPH (**Figure 3**). However, it should be noted that the disruption of the cell wall network did not unequivocally lead to better network forming potential. Indeed, when increasing the pressure level above 20 MPa, G' significantly decreased, but was still significantly higher than before HPH (**Figure 5**). A comparable trend was observed by Augusto et al. (2013b) for tomato juice. These authors also reported that HPH at lower pressure levels (10-50 MPa) had a considerable effect on the microstructure, which resulted in a stronger network, but which could be partially disturbed when applying HPH at higher pressure levels (Augusto et al., 2013a). The additional increase in the accessibility of the cell wall network by using higher pressure levels was probably limited in comparison to what was obtained at 10 and 20 MPa, based on the almost equal WBC over the different pressure levels (**Figure 3**). However, a more extensive particle size reduction, clearly observed with increasing pressure level (**Figure 2**), could decrease the amount of interaction zones on the particles and the potential to form entanglements and, as a consequence, reduce the ability to form a stiff network.

3.3 The effect of method and extent of pectin depletion on the impact of high-pressure homogenization on the microstructural properties of cell wall material

From the previous sections, it is clear that pectin depletion by acid extraction could weaken the cell wall network, which enhanced the potential of HPH to increase the network forming potential of the CWM. In what follows, the role of pectin depletion in the functionalization of CWM by HPH is further elaborated. To gain insight into the effect of both the extent and method of pectin depletion, the effect of HPH on the microstructural and functional properties is compared for the AIR and four UFs obtained after different pectin extraction approaches as outlined in section 2.1 and visualized in **Supplementary Figure 1**. Since

399 the amount of hemicellulose being co-extracted during the extraction approaches applied (even when
400 facilitated by HPH) was negligible (Van Audenhove, Bernaerts, De Smet, et al., 2021), the current study
401 focuses on the specific role of the method and extent of pectin depletion on the WBC and network forming
402 potential of the CWM fractions as well as on the functionalization by HPH at 20 MPa. For this part of the
403 study, HPH was performed at 20 MPa, since the results on the role of pressure level showed that
404 functionalization (at least when the CWM fraction could be functionalized) was optimal around 20 MPa
405 (**Figure 5**).

406 Before HPH, the cell-like morphology of the particles could be recognized for the AIR suspension and for
407 all suspensions of the CWM fractions obtained after each of the solvent-based pectin extractions applied
408 (i.e., the CUF, lAUF and AcUF) (**Figure 6**). Vetter & Kunzek (2003) also observed for apple CWM that
409 (partial) pectin extraction did not have a significant impact on the shape of the original cells. The overall
410 intactness of the cell morphology of the pectin-depleted samples was not substantially changed neither
411 by the use of acid conditions (pH 1.6) combined with high temperature (80 °C), as discussed above, nor
412 by extensive pectin depletion, including the more strongly bound pectin extractable in low-alkaline
413 medium (Fry, 1986). The cell walls in the lAUF consist of the hemicellulose-cellulose network together
414 with a small residual amount of pectin, which is suggested to strongly interact with the hemicellulose-
415 cellulose network (Cosgrove, 2018; Zykwinska et al., 2005). Thus, the strength of this network together
416 with a small amount of residual pectin seemed sufficient to retain the original cell morphology during the
417 Ultra-Turrax mixing as visualized by the microscopic technique used. Furthermore, the PSDs of the UFs
418 prepared by solvent-based pectin extraction (i.e., the CUF, lAUF and AcUF) were almost completely
419 overlaying (**Figure 7A**), which again stipulates that the cell-like morphology was hardly changed by the
420 extraction methods used. These PSDs of the CWM suspensions were all monomodal and their peaks and
421 the corresponding $d_{4,3}$ were around 400 µm (**Figure 7B**).

422 The suspensions (2% w/w) prepared from the AIR and UFs were high-pressure homogenized at 20 MPa.
423 The impact of HPH on the cell walls of the CUF was mainly limited to slight deformation and some
424 breakage (**Figure 6**). The cell-like morphology was mainly retained after HPH at 20 MPa, which is very
425 similar to what was observed for the AIR. Moreover, no difference between the $d_{4,3}$ before and after HPH
426 was observed in the case of the CUF suspension. Interestingly, the PSD was somewhat broader after HPH.
427 The limited increase in particles with smaller size, which was also observed for the AIR, was most likely
428 also the result of some limited breakage of weak cells. Apart from that, also a fraction of particles with
429 larger particle sizes (between 650 – 1300 µm) emerged upon HPH. This increased fraction of particles with

larger sizes could probably be attributed to some stretching of part of the cell walls in the CUF suspension during HPH (**Figure 6**). Although the CUF and AcUF had approximately the same extent of pectin depletion, the pectin-depleted cell walls in the CUF were much less prone to disruption by HPH than the cell walls in the AcUF. This noteworthy difference in susceptibility of the CUF and AcUF stipulates that not only the amount of residual pectin should be considered in this matter but also the type of pectin extracted and the effect of the extraction conditions on the pectin residing in the UF. First of all, it was observed by Van Audenhove, Bernaerts, De Smet, et al. (2021) that the acid extraction resulted in the extraction of pectin which was richer in RG-I (with shorter side chains) than by extraction with hot water followed by extraction with CDTA. Furthermore, for the conditions used to prepare the AcUF, it is known that some hydrolysis of the side-chains could occur (Kaya et al., 2014; Yapo et al., 2007). Considering the recent insights suggesting that the interactions between pectin and the cellulose-hemicellulose network are especially mediated by the pectin side-chains (Zykwinska et al., 2007; Zykwinska et al., 2005), the hydrolysis of these side-chains during the acid extraction could have extensively weakened the interactions within the cell wall and, as a consequence, led to disruption of the cell wall network under the high shear applied by HPH. On the other hand, the conditions used to prepare the CUF are much milder and are expected to have less effect on the chemical structure of the residual pectin. As a consequence, the cell wall network probably had comparable strength as the cell wall in the AIR, explaining the very similar effect on their microstructure upon HPH at 20 MPa.

The cell-like morphology of the lAUF was lost and the CWM was disrupted by HPH at 20 MPa to a continuum of CWM fragments without clear visible cell wall structures, which is comparable to what was observed after homogenization of the AcUF suspension. This is not unexpected, as the cell walls of the lAUF were weakened by the extensive extraction of pectin whereby also the more strongly interacting RG-I rich pectin was extracted (Van Audenhove, Bernaerts, De Smet, et al., 2021). Moreover, demethoxylation and some β-elimination of the pectin are expected to occur at the low-alkaline conditions used during the last step of the lAUF generation (Christiaens et al., 2016). Despite that the lAUF was substantially more pectin-depleted than the AcUF, the shift of the PSD to lower particle sizes was clearly larger for the AcUF than for the lAUF (**Figure 7A**). Based on this quantitative observation, it can be concluded that also the different impact of these pectin extraction conditions on the chemical structure of the residual pectin had a relevant contribution to this difference in cell wall strength. More specifically, the acid hydrolysis of the residual pectin occurring during the AcUF preparation seemed to result in a lower cell wall strength than the impact of the alkaline conditions on the pectin during the lAUF preparation.

The extensively pectin-depleted fraction AcUF-HPH-AcUF did not show the cell-like morphology and was characterized by a $d_{4,3}$ (253 ± 30 µm) which was much lower than the fractions obtained after solvent pectin extraction only. Undeniably, this microstructure is the result of the HPH treatment (also at 20 MPa) preceding the further pectin depletion by subsequent water and acid extraction. However, it is remarkable that the $d_{4,3}$ of the AcUF-HPH-AcUF was in between the values obtained for the AcUF suspension before HPH (393 ± 1 µm) and after HPH (125 ± 5 µm) (**Figure 7B**). The larger particles could also be observed in the micrographs of the AcUF-HPH-AcUF as denser aggregates (**Figure 6**). This peculiar result could be explained as follows. Since the pH during the repeated acid extraction (i.e., 1.6) was far below the pKa of the GalA units of pectin, the material probably aggregated to a certain extent as the repulsive interactions (between charged pectin chains) decreased, while the attractive interactions between the polymers and CWM particles of the disrupted AcUF were still present (e.g., hydrogen bonding, van der Waals forces and hydrophobic interactions) (Kavanagh & Ross-Murphy, 1998; Rao, 2014; Redgwell et al., 2008). Only increasing the pH again to 4.5 during the AcUF-HPH-AcUF suspension preparation and thus reestablishing the repulsive forces did not seem sufficient to completely disturb the aggregates formed. Notwithstanding the further pectin depletion of the AcUF, repeating the high mechanical shear by HPH reduced the particle size only to what was observed after the first homogenization step (**Figure 7**). This implies that probably only one acid extraction already weakened the cell wall (as discussed above) to such an extent that further pectin depletion did not additionally facilitate the HPH-induced disruption of this material.

3.4 The effect of method and extent of pectin depletion on the impact of high-pressure homogenization on the functional properties of cell wall material in suspension

3.4.1 Water binding capacity

In this part, the role of both the extent and method of pectin depletion on the WBC is studied at 2% (w/w). First of all, it can be noted that the values of the WBC of the AIR and AcUF measured at 2% (w/w) (**Figure 8**) were lower than when measured at 1% (w/w) (**Figure 3**). At higher concentration, particles are more in contact with each other (Den Ouden & Van Vliet, 1997), whereas at lower concentration, because of the lower amount of interparticle interactions, it can be expected that more binding spots are available for water resulting in a higher WBC. The WBC of the AIR, CUF and lAUF were almost equal and all substantially lower than the WBC of the AcUF. This is confirmed by the microscopic visualization. In comparison to the cell walls of the AIR, CUF and lAUF, the cell walls of the AcUF seemed to be slightly swollen (**Figure 6**). As the CUF and AcUF were almost equivalently depleted in pectin, composition alone could thus not explain the large difference in the WBC of these fractions. This comparison between the different CWM fractions

indicates that the method and extent of pectin extraction rather than solely the extent of pectin depletion have an effect on the WBC. The harsher conditions to generate the AcUF could lead to a higher disturbance of the cell wall network (e.g., by hydrolyzing the side-chains involved in the interaction with hemicellulose and cellulose) than the milder extraction conditions used for the CUF generation. As a consequence, a higher porosity and accessibility to water of the cell wall structure can thus be expected for the AcUF compared to the CUF.

The low-alkaline conditions during the last step of the stepwise extraction weakened the cell wall by extensive pectin extraction and probably some β-elimination. However, the WBC of the lAUF was clearly lower than the WBC of the AcUF, while for both a porous structure can thus be expected (at least more than for the AIR and CUF). However, not only the porosity of the fibrous system, but also the chemical composition could have an important role in the water binding (Auffret et al., 1994; López et al., 1996). Although the lAUF probably contained more free carboxyl groups (due to the alkaline conditions) on the residual pectin than the AcUF (Christiaens et al., 2016; Willemsen et al., 2017), it is not unreasonable that the higher WBC of the AcUF could be attributed to the higher residual pectin content which could result in an increased WBC because of a higher amount of binding spots available for water. In this context, Auffret et al. (1994) showed that fibers of citrus and sugar beet had a higher WBC than fibers of wheat bran and pea hulls, related to the higher pectin content in the former two matrices, as pectin can bind water to its hydrophilic and charged groups (Chaplin, 2003; Einhorn-Stoll, 2018). Moreover, when more residual pectin is present, the polysaccharide network has a more hydrophilic nature and is suggested to be more expanded (at least when the ionic strength is low) (Auffret et al., 1994). As a consequence, next to the fact that the cell wall network in the lAUF seemed to be less weakened than for the AcUF, the lower WBC of the lAUF than for the AcUF could especially be attributed to the much lower residual pectin content of the lAUF. The non-significant difference in the WBC between the CUF and lAUF despite of the expected difference in porosity could also be explained by the content of the residual pectin.

A significant increase in the WBC by HPH at 20 MPa was observed for the lAUF and AcUF, whereas the effect of HPH was insignificant for the AIR and CUF (**Figure 8**). In line with what was observed for the AIR and AcUF at different pressure levels, an increase in WBC was only observed when the cell wall structure could efficiently be disrupted (i.e., for the lAUF and AcUF) instead of only mainly broken (i.e., for the AIR and CUF). Upon disruption of tomato tissue particles, Lopez-Sanchez, Nijsse, et al. (2011) observed that the phase volume (also determined by centrifugation) of the particles increased by more pronounced swelling. In the dense CWM network, the higher accessibility of the water interaction sites on the CWM

and swelling after HPH likely resulted in the HPH-induced increase in the WBC observed for the lAUF and AcUF. This increase overcompensated the loss of the water entrapped by the cell walls.

The lower WBC (**Figure 8**) of the AcUF-HPH-AcUF before HPH in comparison with the AcUF suspension after HPH showed that the removal of the solubilized and acid extractable pectin after HPH resulted in a decrease in the WBC. Apart from that, the lower WBC could probably also partially be attributed to the reduction in the surface area on the particles available for interaction with water due to the substantial aggregation of the dispersed particles in the AcUF induced by the extraction process as discussed above. Interestingly, the WBC was not significantly increased by HPH, which can be attributed to two factors. First, the beneficial impact of the disruption induced by HPH was more limited than for the AcUF, since the microstructure of the AcUF-HPH-AcUF had already a certain disrupted nature. Second, the residual pectin content of the AcUF-HPH-AcUF was clearly lower than for the AcUF. In this regard, it is reasonable that the WBC of the homogenized lAUF and the homogenized AcUF-HPH-AcUF (both rather extensively pectin-depleted) was very similar.

3.4.2 Viscoelastic properties

In order to address the role of the extent and method of pectin depletion on the network forming potential of the CWM, the G' of the AIR, CUF, lAUF and AcUF suspensions at 2% (w/w) concentration was compared (**Figure 9**). The high values of the G' for the AIR and the UFs suspensions could be attributed to an elastic network formed by the close packing of the intact (partially or extensively pectin-depleted) cell walls (Leverrier et al., 2021; Lopez-Sanchez et al., 2012). When comparing the G' of the AIR and AcUF suspensions before HPH between the two concentrations used (1% versus 2%), the G' of the suspensions at 2% was, as expected, much higher. Indeed, a higher concentration favors a closer packing of the cell-like particles resulting in a stronger network (Lopez-Sanchez et al., 2012).

The relation between the G' and G" [Pa] and the angular frequency [rad/s] is shown in **Supplementary Figure 3** for each of the suspensions prepared from the AIR and the UFs before and after HPH. A similar dependency of the G' and G" on the angular frequency was observed in **Supplementary Figure 2**. Even before HPH, the range of the G' values obtained before HPH was rather broad, namely from 780 to 1461 Pa (**Figure 9**). Based on the G' of their suspensions, two groups could be discerned over the CWM fractions studied. The G' of the suspensions prepared with the AIR and lAUF were around 750 to 900 Pa, whereas for the CUF and AcUF suspensions a clearly higher value was observed, namely around 1350 to 1500 Pa. However, neither the general microstructure, as the AIR, CUF, lAUF and AcUF were all characterized by intact (partially or extensively pectin-depleted) cell walls, nor the WBC could explain the difference

between the G' of these two groups defined above. Interestingly, it seems that a certain optimal pectin depletion of the CWM exists in the context of its use as a texturizing agent. Indeed, CWM which was partially (around half) pectin-depleted, i.e., the CUF and AcUF, had a higher G' than CWM which was not pectin-depleted (i.e., the AIR) and extensively pectin-depleted (i.e., the lAUF). This trend was different to what has been observed for the CWM of lemon peel, for which an increase in the G' was found with increasing pectin depletion (Willemsen et al., 2017). The G' for 2% (w/w) suspension in standardized tap water of the UFs of lemon peel CWM after pectin extraction with chelator, acid and low-alkaline medium were less than 1 Pa, 38 Pa and around 70 Pa, respectively (Willemsen et al., 2017). These values were also much lower than what was observed for the respective CWM fractions in this study. It is known that the network forming potential of CWM of different botanical origin can highly differ (Redgwell et al., 2008; Van Audenhove, Bernaerts, Putri, et al., 2021). In particular, the size of the particles of tomato CWM was higher than for lemon peel CWM reported by Willemsen et al. (2017).

The critical strain of the AIR and CUF suspensions was higher after HPH at 20 MPa (**Figure 10**). The rigidity of these cell walls was probably lower after HPH due to the limited breakage and deformation of the cell walls (**Figure 6**), which could result in a network with a higher capacity to withstand against the applied shear. Although the critical strain of the lAUF, AcUF and AcUF-HPH-AcUF suspension increased by high-pressure homogenization, the value for the homogenized AcUF suspension was substantially higher than the values obtained for the homogenized lAUF and AcUF-HPH-AcUF suspensions. This observation highlights the possible role of residual pectin in increasing the strength of the network formed by CWM which is efficiently disrupted by HPH, most probably because of the effect of pectin on the interactions between the cell wall fragments (Beresovsky et al., 1995) and the possibility to form polymer entanglements (Lopez-Sanchez & Farr, 2012).

The effect of HPH on G' of the suspensions was highly differing among the CWM fractions studied (**Figure 9**). While HPH had a negative effect on the G' of the AIR and CUF suspensions, a clear increase in the G' was observed for the lAUF and AcUF suspensions. It was already discussed above that the non-pectin-depleted CWM, represented by the AIR, could not be functionalized even when using very high pressure levels (up to 80 MPa). Based on the results for the CUF at 20 MPa, it is clear that also partial pectin depletion of CWM under mild conditions does not favor the disruption of the CWM above breakage during the HPH treatment. Although the cell-like morphology of both the AIR and the CUF was retained after HPH at 20 MPa, it should be noted that some limited breakage and/or some deformation occurred, which probably resulted in a lower rigidity of these cell walls. It is reasonable that this impact of HPH on the cell

wall had a substantial negative effect on the stiffness of the network, especially as it is formed by the close packing of these cell-like particles. In a less concentrated regime (e.g., at 1% w/w) when the particles are thus less constrained in the volume spanning network, this impact of HPH had no significant effect on the G' of the AIR suspension (**Figure 5**).

Efficient disruption of the CWM by HPH can occur when the interfibrillar interactions can be overcome which can be enhanced by the removal of pectin (Willemsen et al., 2017). In the case of tomato, extensive disruption of the material favored the interaction with water and the formation of other interactions and entanglements between the cell wall fragments than possible between the intact cell-like particles (Lopez-Sanchez, Nijsse, et al., 2011; Lopez-Sanchez & Farr, 2012). When considering the different effect of HPH on the CUF and the AcUF, it is clear that the potential of HPH to increase the network forming potential of the CWM was not only related with the amount of residual pectin. Pectin extraction could only enhance the functionalization by HPH (as observed for the lAUF and AcUF) on the condition that the network was sufficiently weakened. In the context of the functionalization of partially pectin-depleted CWM, this was not only reached by the extraction of pectin as such but also by the chemical reactions occurring due to the conditions applied (e.g., acid hydrolysis of the pectin side-chains). The importance of the latter factor was clearly shown by the difference in the potential of HPH to functionalize the CUF and AcUF.

In contrast to before HPH, a clear linear relation existed after HPH between the WBC of the CWM suspensions and the G' of the respective suspensions (both assessed at 2% w/w) (**Figure 11**). When the WBC of the suspension was higher, the G' was higher. By Willemsen, Panozzo, Moelants, Wallecan, & Hendrickx (2020), it was shown for the residue after acid pectin extraction from the AIR of lemon peel that a clear relation existed between the swelling volume of the material and the G' of the suspensions, depending on the pre-treatments and the application of HPH. Also for pumpkin pomace suspensions with different composition, a linear correlation was found between the swelling volume and the G' (Atencio et al., 2021).

In the current study, a prominent role of pectin in the rheological properties of partially and extensively pectin-depleted CWM suspensions which are efficiently disrupted by HPH is shown. Indeed, the high-pressure homogenized AcUF suspension was characterized by both the highest stiffness (i.e., G') as well as the highest strength (critical strain). As was described by Van Audenhove, Bernaerts, De Smet, et al. (2021), cell wall polysaccharides, pectin in particular, could be released into the serum phase during HPH of the AcUF suspensions. When more pectin is present in the serum phase, its viscosity is higher (Moelants et al., 2013) and the interaction between particles could be enhanced (Beresovsky et al., 1995).

Nevertheless, the role of the particle phase should not be underestimated, as research on tomato-based systems containing both soluble polymers (pectin) in the serum phase as well as a particle phase showed that the role of the particles in determining the overall viscosity or consistency was higher than the role of the soluble polymers (Fei et al., 2021; Palmero et al., 2016; Santiago et al., 2017). However, when the solubilized and more accessible pectin was removed by repeated acid extraction from the high-pressure homogenized AcUF, the G' clearly decreased from 1808 ± 94 Pa observed for the AcUF to 726 ± 201 Pa for the AcUF-HPH-AcUF (**Figure 9**). However, it should be noted that this decrease was not only the result of the further pectin extraction but also of the aggregation of the material which could significantly reduce the amount of interactions. Indeed, HPH of the AcUF-HPH-AcUF reestablished the same extent of particle disruption as for the AcUF, clearly increasing the G' of the AcUF-HPH-AcUF suspension. Nevertheless, the G' and the WBC of the AcUF-HPH-AcUF after HPH was in between the values obtained for the AcUF and lAUF suspensions after HPH. Based on these observations, the role of the pectin in the texturizing properties of high-pressure homogenized CWM suspensions is twofold. On the one hand, a certain extent of pectin extraction is needed (together with extraction conditions which have a weakening effect on the cell wall structure) to enhance the disruption of the original microstructure by HPH to form new interactions leading to a stiffer network. On the other hand, the residual pectin in the disrupted homogenized suspensions (i.e., the lAUF, AcUF and AcUF-HPH-AcUF after HPH) has a substantial role in reaching a higher WBC and in creating a stiff and strong network in these homogenized systems.

4 Conclusions

The role of pectin depletion in enhancing the functionalization of CWM by HPH was assessed in a study on tomato. Apart from a slightly higher particle size observed for the AIR suspension, the microstructure of all non-high-pressure homogenized CWM fractions was characterized by cell-like particles. Thus, neither the extent nor the method of pectin depletion among the solvent-based extraction approaches used altered the cell shape. The effect of pectin extraction became prominent upon disruption by HPH. HPH of the AIR mainly resulted in breakage of the cell walls, especially at higher pressure levels. On the other hand, HPH of the AcUF resulted in the disruption of the cell wall network. Increasing the pressure level applied during HPH of the AIR resulted in further particle size reduction but mainly by more extensive breakage and not by disruption of the cell wall network as observed for the AcUF. Although the CUF was partially pectin-depleted like the AcUF, HPH at 20 MPa on the CUF only resulted in some breakage and deformation. This result showed that only extracting half of the original amount of pectin was not sufficient to enable efficient disruption during HPH. Interestingly, also further weakening of the cell wall

by altering the chemical structure of the residual pectin (in this case mainly acid hydrolysis of the pectin side-chains) due to the conditions during the extraction was needed. On the other hand, the lAUF was also disrupted by HPH at 20 MPa similar to what was observed for the AcUF, which could be attributed to the high extent of pectin-depletion and probably some β-elimination occurring under the low-alkaline conditions.

Before HPH, CWM with intermediate level of pectin depletion had the greatest network forming potential, since the G' of the suspensions prepared with partially pectin-depleted CWM (i.e., the CUF or AcUF) was higher than for the suspensions prepared with the AIR or extensively pectin-depleted CWM (i.e., the lAUF). The differences in impact of HPH on the microstructure showed to have important repercussions on the resulting stiffness of the suspensions. The WBC as well as the network stiffness of the lAUF and AcUF was increased by HPH. This was attributed to the significant disruptive effect of HPH (at 20 MPa) on the intact pectin-depleted cell walls, consequently resulting in the formation of new interactions between fragments and released polymers (especially pectin) and in a network more accessible for the interaction with water. On the other hand, for the AIR and CUF suspensions, on which the impact of HPH at 20 MPa was limited to slight disruption of the CWM, a decrease in the network stiffness was observed, probably due to the lower rigidity of the cell walls in the packed network after being subjected to HPH. The current results show that pectin extraction can enhance the functionalization of CWM by HPH provided that the extent and conditions during extraction resulted in sufficient weakening of the cell wall to enable an efficient disruption during HPH. However, a higher residual pectin content in the suspensions of disrupted CWM obtained after HPH resulted in a higher WBC and higher network stiffness. Furthermore, after HPH at 20 MPa, a strong positive correlation between the WBC and the stiffness of the suspension of the respective CWM fraction was observed.

Since the results showed that the pectin depletion level and method determined not only the water binding and the rheological properties of the CWM in model suspensions but also the potential of HPH to generate a microstructure with increased network forming potential, which is expected to be desirable when the material would be used as texturizing agent, the current study could serve as a starting point for more application-oriented research aiming to unravel the possible applications of fruit and vegetable CWM (maybe even from tissues obtained as waste or side-stream) in real food products. Furthermore, research specifically addressing the role of hemicellulose in the functional properties of (extensively pectin-depleted) CWM fractions could be an interesting next step to gain further insight into the relation between composition of the CWM and its functionality.

Acknowledgements

J. Van Audenhove is a PhD fellow funded by the Research Foundation Flanders (FWO), grant number 1134619N. T. Bernaerts is a postdoctoral researcher funded by the Research Foundation Flanders (FWO), grant number 1252221N. The funding source had no role in the study design, collection, analysis and interpretation of the data, the writing of this manuscript or in the decision to submit the manuscript for publication.

References

Appelqvist, I. A. M., Cochet-Broch, M., Poelman, A. A. M., & Day, L. (2015). Morphologies, volume fraction and viscosity of cell wall particle dispersions particle related to sensory perception. *Food Hydrocolloids*, *44*, 198–207. https://doi.org/10.1016/j.foodhyd.2014.09.012

Atencio, S., Bernaerts, T., Liu, D., Reineke, K., Hendrickx, M., & Van Loey, A. (2021). Impact of processing on the functionalization of pumpkin pomace as a food texturizing ingredient. *Innovative Food Science & Emerging Technologies*, *69*, 102669. https://doi.org/10.1016/j.ifset.2021.102669

Auffret, A., Ralet, M.-C., Guillon, F., Barry, J.-L., & Thibault, J.-F. (1994). Effect of Grinding and Experimental Conditions on the Measurement of Hydration Properties of Dietary Fibres. *LWT - Food Science and Technology*, *27*(2), 166–172. https://doi.org/10.1006/fstl.1994.1033

Augusto, P. E. D., Ibarz, A., & Cristianini, M. (2013a). Effect of high pressure homogenization (HPH) on the rheological properties of tomato juice: Viscoelastic properties and the Cox-Merz rule. *Journal of Food Engineering*, *114*(1), 57–63. https://doi.org/10.1016/j.jfoodeng.2012.07.025

Augusto, P. E. D., Ibarz, A., & Cristianini, M. (2013b). Effect of high pressure homogenization (HPH) on the rheological properties of tomato juice: Creep and recovery behaviours. *Food Research International*, *54*(1), 169–176. https://doi.org/10.1016/j.foodres.2013.06.027

Bayod, E., Månsson, P., Innings, F., Bergenståhl, B., & Tornberg, E. (2007). Low Shear Rheology of Concentrated Tomato Products. Effect of Particle Size and Time. *Food Biophysics*, *2*(4), 146–157. https://doi.org/10.1007/s11483-007-9039-2

Bayod, E., & Tornberg, E. (2011). Microstructure of highly concentrated tomato suspensions on homogenisation and subsequent shearing. *Food Research International*, *44*(3), 755–764. https://doi.org/10.1016/j.foodres.2011.01.005

Bayod, E., Willers, E. P., & Tornberg, E. (2008). Rheological and structural characterization of tomato paste and its influence on the quality of ketchup. *LWT - Food Science and Technology*, *41*(7), 1289–1300. https://doi.org/10.1016/j.lwt.2007.08.011

Becker, R., Miers, J. C., Nutting, M.-D., Dietrich, W. C., & Wagner, J. R. (1972). Consistency of tomato products. 7. Effects of acidification on cell walls and cell breakage. *Journal of Food Science*, *37*(1), 118–125. https://doi.org/10.1111/j.1365-2621.1972.tb03399.x

Bengtsson, H., & Tornberg, E. (2011). Physicochemical characterization of fruit and vegetable fiber suspensions. I: effect of homogenization. *Journal of Texture Studies*, *42*(4), 268–280. https://doi.org/10.1111/j.1745-4603.2010.00275.x

Beresovsky, N., Kopelman, I. J., & Mizrahi, S. (1995). The role of pulp interparticle interaction in determining tomato juice viscosity. *Journal of Food Processing and Preservation*, *19*(2), 133–146. https://doi.org/10.1111/j.1745-4549.1995.tb00283.x

Burton, R. A., Gidley, M. J., & Fincher, G. B. (2010). Heterogeneity in the chemistry, structure and function of plant cell walls. *Nature Chemical Biology*, *6*(10), 724–732. https://doi.org/10.1038/nchembio.439

Carpita, N. C., & Gibeaut, D. M. (1993). Structural models of primary cell walls in flowering plants: consistency of molecular structure with the physical properties of the walls during growth. *The Plant Journal*, *3*(1), 1–30. https://doi.org/10.1111/j.1365-313X.1993.tb00007.x

Carpita, N., Sabularse, D., Montezinos, D., & Delmer, D. P. (1979). Determination of the Pore Size of Cell Walls of Living Plant Cells. *Science*, *205*(4411), 1144–1147. https://doi.org/10.1126/science.205.4411.1144

Chaplin, M. F. (2003). Fibre and water binding. *Proceedings of the Nutrition Society*, *62*(1), 223–227. https://doi.org/10.1079/PNS2002203

Christiaens, S., Van Buggenhout, S., Houben, K., Jamsazzadeh Kermani, Z., Moelants, K. R. N., Ngouémazong, E. D., Van Loey, A., & Hendrickx, M. E. G. (2016). Process–Structure–Function Relations of Pectin in Food. *Critical Reviews in Food Science and Nutrition*, *56*(6), 1021–1042. https://doi.org/10.1080/10408398.2012.753029

Cosgrove, D. J. (2001). Wall Structure and Wall Loosening. A Look Backwards and Forwards. *Plant Physiology*, *125*(1), 131–134. https://doi.org/10.1104/pp.125.1.131

Cosgrove, D. J. (2014). Re-constructing our models of cellulose and primary cell wall assembly. *Current Opinion in Plant Biology*, *22*, 122–131. https://doi.org/10.1016/j.pbi.2014.11.001

Cosgrove, D. J. (2018). Diffuse Growth of Plant Cell Walls. *Plant Physiology*, *176*(1), 16–27. https://doi.org/10.1104/pp.17.01541

Daher, F. B., & Braybrook, S. A. (2015). How to let go: pectin and plant cell adhesion. *Frontiers in Plant Science*, *6*, 523–530. https://doi.org/10.3389/fpls.2015.00523

Day, L., Xu, M., Øiseth, S. K., Hemar, Y., & Lundin, L. (2010). Control of morphological and rheological properties of carrot cell wall particle dispersions through processing. *Food and Bioprocess Technology*, *3*(6), 928–934. https://doi.org/10.1007/s11947-010-0346-0

Del Valle, M., Cámara, M., & Torija, M.-E. (2006). Chemical characterization of tomato pomace. *Journal of the Science of Food and Agriculture*, *86*(8), 1232–1236. https://doi.org/10.1002/jsfa.2474

Den Ouden, F. W. C., & Van Vliet, T. (1997). Particle Size Distribution in Tomato Concentrate and Effects on Rheological Properties. *Journal of Food Science*, *62*(3), 565–567. https://doi.org/10.1111/j.1365-2621.1997.tb04431.x

Doblin, M. S., Pettolino, F., & Bacic, A. (2010). Plant cell walls: the skeleton of the plant world. *Functional Plant Biology*, *37*(5), 357. https://doi.org/10.1071/FP09279

Einhorn-Stoll, U. (2018). Pectin-water interactions in foods – From powder to gel. *Food Hydrocolloids*, *78*, 109–119. https://doi.org/10.1016/j.foodhyd.2017.05.029

Fei, X., Jones, O. G., Reuhs, B. L., & Campanella, O. H. (2021). Soluble pectin acts as a particle stabilizer of tomato suspensions: The impact on tomato products rheological characterization. *LWT*, *139*,

110508. https://doi.org/10.1016/j.lwt.2020.110508

Foster, T. J. (2011). Natural structuring with cell wall materials. *Food Hydrocolloids*, *25*(8), 1828–1832. https://doi.org/10.1016/j.foodhyd.2011.05.016

Fry, S. C. (1986). Cross-Linking of Matrix Polymers in the Growing Cell Walls of Angiosperms. *Annual Review of Plant Physiology*, *37*(1), 165–186. https://doi.org/10.1146/annurev.pp.37.060186.001121

Gundurao, A., Ramaswamy, H. S., & Ahmed, J. (2011). Effect of soluble solids concentration and temperature on thermo-physical and rheological properties of mango puree. *International Journal of Food Properties*, *14*(5), 1018–1036. https://doi.org/10.1080/10942910903580876

Jarvis, M. C. (2011). Plant cell walls: Supramolecular assemblies. *Food Hydrocolloids*, *25*(2), 257–262. https://doi.org/10.1016/j.foodhyd.2009.09.010

Kaur, G. J., Orsat, V., & Singh, A. (2021). An overview of different homogenizers, their working mechanisms and impact on processing of fruits and vegetables. *Critical Reviews in Food Science and Nutrition*, *0*(0), 1–14. https://doi.org/10.1080/10408398.2021.1969890

Kavanagh, G. M., & Ross-Murphy, S. B. (1998). Rheological characterisation of polymer gels. *Progress in Polymer Science*, *23*(3), 533–562. https://doi.org/10.1016/S0079-6700(97)00047-6

Kaya, M., Sousa, A. G., Crépeau, M.-J., Sørensen, S. O., & Ralet, M.-C. (2014). Characterization of citrus pectin samples extracted under different conditions: influence of acid type and pH of extraction. *Annals of Botany*, *114*(6), 1319–1326. https://doi.org/10.1093/aob/mcu150

Khan, M. I. H., Wellard, R. M., Nagy, S. A., Joardder, M. U. H., & Karim, M. A. (2016). Investigation of bound and free water in plant-based food material using NMR T2 relaxometry. *Innovative Food Science & Emerging Technologies*, *38*, 252–261. https://doi.org/10.1016/j.ifset.2016.10.015

Kotcharian, A., Kunzek, H., & Dongowski, G. (2004). The influence of variety on the enzymatic degradation of carrots and on functional and physiological properties of the cell wall materials. *Food Chemistry*, *87*(2), 231–245. https://doi.org/10.1016/j.foodchem.2003.11.015

Kubo, M. T. K., Augusto, P. E. D., & Cristianini, M. (2013). Effect of high pressure homogenization (HPH) on the physical stability of tomato juice. *Food Research International*, *51*(1), 170–179. https://doi.org/10.1016/j.foodres.2012.12.004

Kunzek, H., Kabbert, R., & Gloyna, D. (1999). Aspects of material science in food processing: changes in plant cell walls of fruits and vegetables. *Zeitschrift Für Lebensmitteluntersuchung Und -Forschung A*, *208*(4), 233–250. https://doi.org/10.1007/s002170050410

Leverrier, C., Almeida, G., Cuvelier, G., & Menut, P. (2021). Modelling shear viscosity of soft plant cell suspensions. *Food Hydrocolloids*, *118*, 106776. https://doi.org/10.1016/j.foodhyd.2021.106776

Leverrier, C., Almeida, G., Espinosa-Muñoz, L., & Cuvelier, G. (2016). Influence of Particle Size and Concentration on Rheological Behaviour of Reconstituted Apple Purees. *Food Biophysics*, *11*(3), 235–247. https://doi.org/10.1007/s11483-016-9434-7

Levy, R., Okun, Z., & Shpigelman, A. (2020). High-Pressure Homogenization: Principles and Applications Beyond Microbial Inactivation. *Food Engineering Reviews*. https://doi.org/10.1007/s12393-020-09239-8

Lopez-Sanchez, P., Chapara, V., Schumm, S., & Farr, R. (2012). Shear Elastic Deformation and Particle

Packing in Plant Cell Dispersions. *Food Biophysics*, *7*(1), 1–14. https://doi.org/10.1007/s11483-011-9237-9

Lopez-Sanchez, P., & Farr, R. (2012). Power Laws in the Elasticity and Yielding of Plant Particle Suspensions. *Food Biophysics*, *7*(1), 15–27. https://doi.org/10.1007/s11483-011-9238-8

Lopez-Sanchez, P., Nijsse, J., Blonk, H. C. G., Bialek, L., Schumm, S., & Langton, M. (2011). Effect of mechanical and thermal treatments on the microstructure and rheological properties of carrot, broccoli and tomato dispersions. *Journal of the Science of Food and Agriculture*, *91*(2), 207–217. https://doi.org/10.1002/jsfa.4168

Lopez-Sanchez, P., Svelander, C., Bialek, L., Schumm, S., & Langton, M. (2011). Rheology and Microstructure of Carrot and Tomato Emulsions as a Result of High-Pressure Homogenization Conditions. *Journal of Food Science*, *76*(1), E130–E140. https://doi.org/10.1111/j.1750-3841.2010.01894.x

López, G., Ros, G., Rincón, F., Periago, M. J., Martínez, M. C., & Ortuño, J. (1996). Relationship between Physical and Hydration Properties of Soluble and Insoluble Fiber of Artichoke. *Journal of Agricultural and Food Chemistry*, *44*(9), 2773–2778. https://doi.org/10.1021/jf9507699

Lu, Z., Wang, J., Gao, R., Ye, F., & Zhao, G. (2019). Sustainable valorisation of tomato pomace: A comprehensive review. *Trends in Food Science & Technology*, *86*(February), 172–187. https://doi.org/10.1016/j.tifs.2019.02.020

McCann, T. H., Fabre, F., & Day, L. (2011). Microstructure, rheology and storage stability of low-fat yoghurt structured by carrot cell wall particles. *Food Research International*, *44*(4), 884–892. https://doi.org/10.1016/j.foodres.2011.01.045

Moelants, K. R. N., Cardinaels, R., Jolie, R. P., Verrijssen, T. A. J., Van Buggenhout, S., Van Loey, A. M., Moldenaers, P., & Hendrickx, M. E. (2014). Rheology of Concentrated Tomato-Derived Suspensions: Effects of Particle Characteristics. *Food and Bioprocess Technology*, *7*(1), 248–264. https://doi.org/10.1007/s11947-013-1070-3

Moelants, K. R. N., Cardinaels, R., Van Buggenhout, S., Van Loey, A. M., Moldenaers, P., & Hendrickx, M. E. (2014). A Review on the relationships between processing, food structure, and rheological properties of plant-tissue-based food suspensions. *Comprehensive Reviews in Food Science and Food Safety*, *13*(3), 241–260. https://doi.org/10.1111/1541-4337.12059

Moelants, K. R. N., Jolie, R. P., Palmers, S. K. J., Cardinaels, R., Christiaens, S., Van Buggenhout, S., Van Loey, A. M., Moldenaers, P., & Hendrickx, M. E. (2013). The Effects of Process-Induced Pectin Changes on the Viscosity of Carrot and Tomato Sera. *Food and Bioprocess Technology*, *6*, 2870–2883. https://doi.org/10.1007/s11947-012-1004-5

Müller, S., & Kunzek, H. (1998). Material properties of processed fruit and vegetables I. Effect of extraction and thermal treatment on apple parenchyma. *Zeitschrift Für Lebensmitteluntersuchung Und - Forschung A*, *206*(4), 264–272. https://doi.org/10.1007/s002170050255

Palmero, P., Panozzo, A., Colle, I., Chigwedere, C., Hendrickx, M., & Van Loey, A. (2016). Role of structural barriers for carotenoid bioaccessibility upon high pressure homogenization. *Food Chemistry*, *199*, 423–432. https://doi.org/10.1016/j.foodchem.2015.12.062

Rao, M. A. (2014). *Rheology of Fluid, Semisolid, and Solid Foods* (G. V. Barbosa-Canovas (ed.); 3rd ed). Springer US. https://doi.org/10.1007/978-1-4614-9230-6

Redgwell, R. J., Curti, D., & Gehin-Delval, C. (2008). Physicochemical properties of cell wall materials from apple, kiwifruit and tomato. *European Food Research and Technology*, *227*(2), 607–618. https://doi.org/10.1007/s00217-007-0762-1

Sankaran, A. K., Nijsse, J., Bialek, L., Bouwens, L., Hendrickx, M. E., & Van Loey, A. M. (2015). Effect of enzyme homogenization on the physical properties of carrot cell wall suspensions. *Food and Bioprocess Technology*, *8*(6), 1377–1385. https://doi.org/10.1007/s11947-015-1481-4

Santiago, J. S. J., Kermani, Z. J., Xu, F., Van Loey, A. M., & Hendrickx, M. E. (2017). The effect of high pressure homogenization and endogenous pectin-related enzymes on tomato purée consistency and serum pectin structure. *Innovative Food Science & Emerging Technologies*, *43*, 35–44. https://doi.org/10.1016/j.ifset.2017.07.028

Steffe, J. F. (1996). *Rheological methods in food process engineering* (2nd ed). Freeman Press.

Tan, J., & Kerr, W. L. (2015). Rheological properties and microstructure of tomato puree subject to continuous high pressure homogenization. *Journal of Food Engineering*, *166*, 45–54. https://doi.org/10.1016/j.jfoodeng.2015.05.025

Thebaudin, J. Y., Lefebvre, A. C., Harrington, M., & Bourgeois, C. M. (1997). Dietary fibres: Nutritional and technological interest. *Trends in Food Science & Technology*, *8*(2), 41–48. https://doi.org/10.1016/S0924-2244(97)01007-8

Ulbrich, M., & Flöter, E. (2014). Impact of high pressure homogenization modification of a cellulose based fiber product on water binding properties. *Food Hydrocolloids*, *41*, 281–289. https://doi.org/10.1016/j.foodhyd.2014.04.020

Van Audenhove, J., Bernaerts, T., De Smet, V., Delbaere, S., Van Loey, A. M., & Hendrickx, M. E. (2021). The Structure and Composition of Extracted Pectin and Residual Cell Wall Material from Processing Tomato: The Role of a Stepwise Approach versus High-Pressure Homogenization-Facilitated Acid Extraction. *Foods*, *10*(5), 1064. https://doi.org/10.3390/foods10051064

Van Audenhove, J., Bernaerts, T., Putri, N. I., Okello, E. O., Van Rooy, L., Van Loey, A. M., & Hendrickx, M. E. (2021). Microstructural and Texturizing Properties of Partially Pectin-Depleted Cell Wall Material: The Role of Botanical Origin and High-Pressure Homogenization. *Foods*, *10*(11), 2644. https://doi.org/10.3390/foods10112644

Van Buggenhout, S., Wallecan, J., Christiaens, S., Debon, S. J. J., Desmet, C., Van Loey, A., Hendrickx, M., & Mazoyer, J. (2015). Influence of high-pressure homogenization on functional properties of orange pulp. *Innovative Food Science and Emerging Technologies*, *30*, 51–60. https://doi.org/10.1016/j.ifset.2015.05.004

Vetter, S., & Kunzek, H. (2003a). The influence of the pre-drying treatment on the hydration properties of dried cell wall materials from apples. *European Food Research and Technology*, *216*(2), 129–137. https://doi.org/10.1007/s00217-002-0616-9

Vetter, S., & Kunzek, H. (2003b). The influence of the sequential extractions on the structure and the properties of single cell materials from apples. *European Food Research and Technology*, *217*(5), 392–400. https://doi.org/10.1007/s00217-003-0767-3

Waldron, K.W., Parker, M. L., & Smith, A. C. (2003). Plant Cell Walls and Food Quality. *Comprehensive Reviews in Food Science and Food Safety*, *2*(4), 128–146. https://doi.org/10.1111/j.1541-4337.2003.tb00019.x

875 Waldron, Keith W., Smith, A. C., Parr, A. J., Ng, A., & Parker, M. L. (1997). New approaches to
876 understanding and controlling cell separation in relation to fruit and vegetable texture. *Trends in*
877 *Food Science & Technology*, *8*(7), 213–221. https://doi.org/10.1016/S0924-2244(97)01052-2

878 Wang, Y., Sun, P., Li, H., Adhikari, B. P., & Li, D. (2018). Rheological Behavior of Tomato Fiber Suspensions
879 Produced by High Shear and High Pressure Homogenization and Their Application in Tomato
880 Products. *International Journal of Analytical Chemistry*, Article ID 5081938.
881 https://doi.org/10.1155/2018/5081938

882 Willemsen, K. L. D. D., Panozzo, A., Moelants, K., Cardinaels, R., Wallecan, J., Moldenaers, P., & Hendrickx,
883 M. (2018). Effect of pH and salts on microstructure and viscoelastic properties of lemon peel acid
884 insoluble fiber suspensions upon high pressure homogenization. *Food Hydrocolloids*, *82*, 144–154.
885 https://doi.org/10.1016/j.foodhyd.2018.04.005

886 Willemsen, K. L. D. D., Panozzo, A., Moelants, K., Debon, S. J. J., Desmet, C., Cardinaels, R., Moldenaers,
887 P., Wallecan, J., & Hendrickx, M. E. G. (2017). Physico-chemical and viscoelastic properties of high
888 pressure homogenized lemon peel fiber fraction suspensions obtained after sequential pectin
889 extraction. *Food Hydrocolloids*, *72*, 358–371. https://doi.org/10.1016/j.foodhyd.2017.06.020

890 Willemsen, K. L. D. D., Panozzo, A., Moelants, K., Wallecan, J., & Hendrickx, M. (2020). Towards improved
891 understanding of the viscoelastic properties of functionalized lemon peel fibers in suspension based
892 on microstructure, hydration value and swelling volume. *Journal of Food Engineering*, *278*, 109950.
893 https://doi.org/10.1016/j.jfoodeng.2020.109950

894 Yapo, B. M., Robert, C., Etienne, I., Wathelet, B., & Paquot, M. (2007). Effect of extraction conditions on
895 the yield, purity and surface properties of sugar beet pulp pectin extracts. *Food Chemistry*, *100*(4),
896 1356–1364. https://doi.org/10.1016/j.foodchem.2005.12.012

897 Zykwinska, A., Gaillard, C., Buléon, A., Pontoire, B., Garnier, C., Thibault, J.-F., & Ralet, M.-C. (2007).
898 Assessment of In Vitro Binding of Isolated Pectic Domains to Cellulose by Adsorption Isotherms,
899 Electron Microscopy, and X-ray Diffraction Methods. *Biomacromolecules*, *8*(1), 223–232.
900 https://doi.org/10.1021/bm060292h

901 Zykwinska, A. W., Ralet, M.-C. J., Garnier, C. D., & Thibault, J.-F. J. (2005). Evidence for In Vitro Binding of
902 Pectin Side Chains to Cellulose. *Plant Physiology*, *139*(1), 397–407.
903 https://doi.org/10.1104/pp.105.065912

904

905

Pressure level	AIR	AcUF
0 MPa	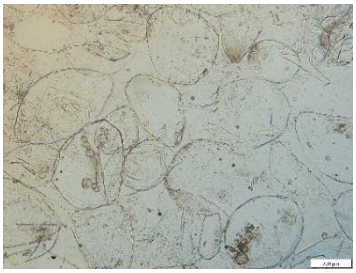	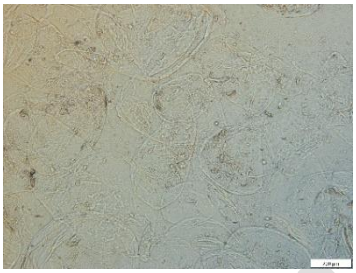
10 MPa		
20 MPa		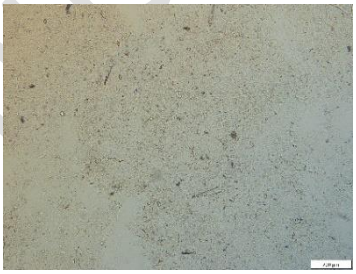
40 MPa	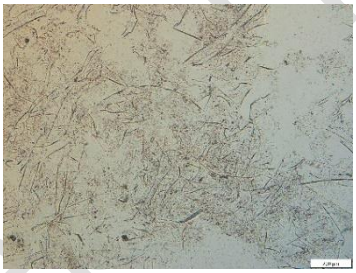	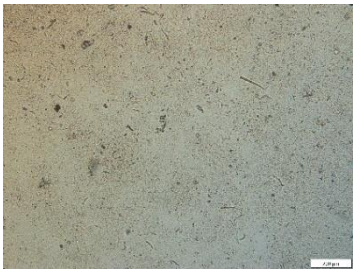
60 MPa		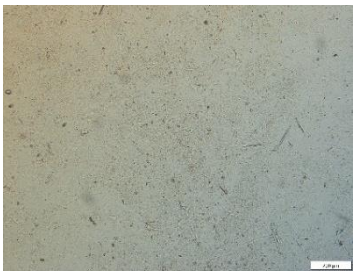

80 MPa

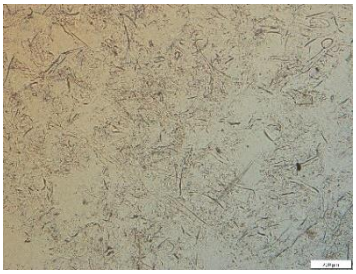

906

907 **Figure 1**: Microscopic visualization of the suspensions prepared with the alcohol-insoluble residue (AIR)
908 or the acid-unextractable fraction (AcUF) at 0.6% (w/w) concentration before (0 MPa) and after high-
909 pressure homogenization (performed at 1% w/w) at different pressure levels. Scale bar represents 200
910 µm.

911

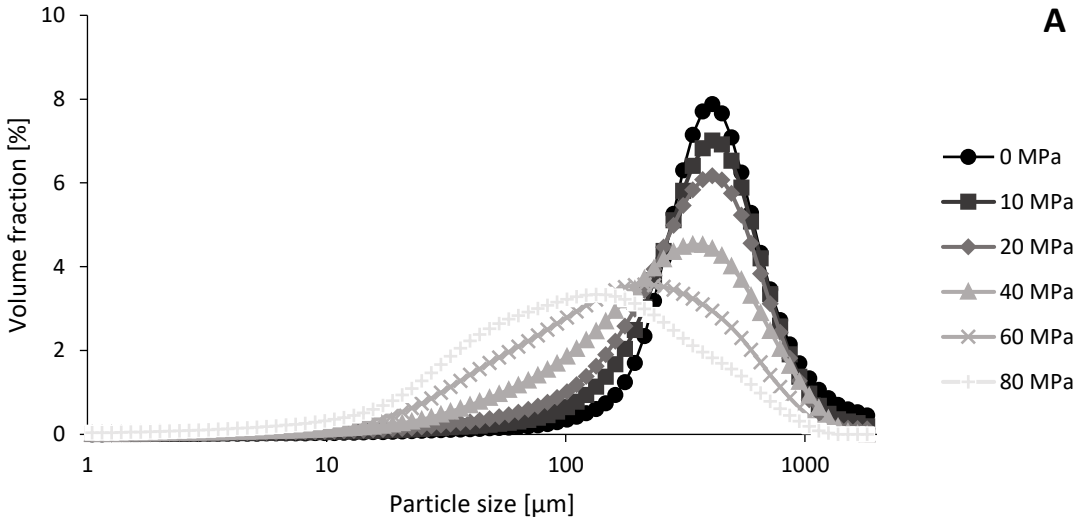
A
Volume fraction [%]
Particle size [µm]
0 MPa
10 MPa
20 MPa
40 MPa
60 MPa
80 MPa

912

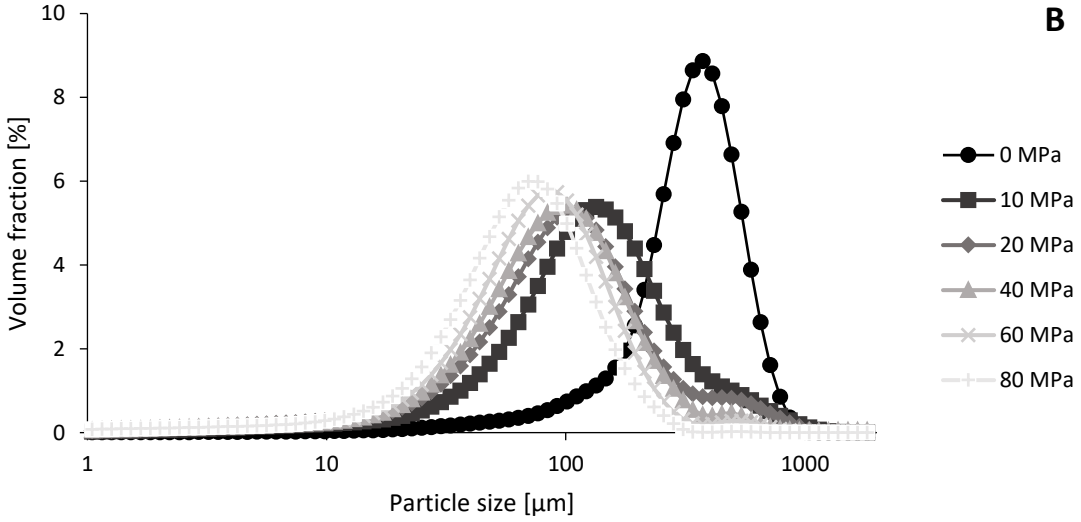
B
Volume fraction [%]
Particle size [µm]
0 MPa
10 MPa
20 MPa
40 MPa
60 MPa
80 MPa

913

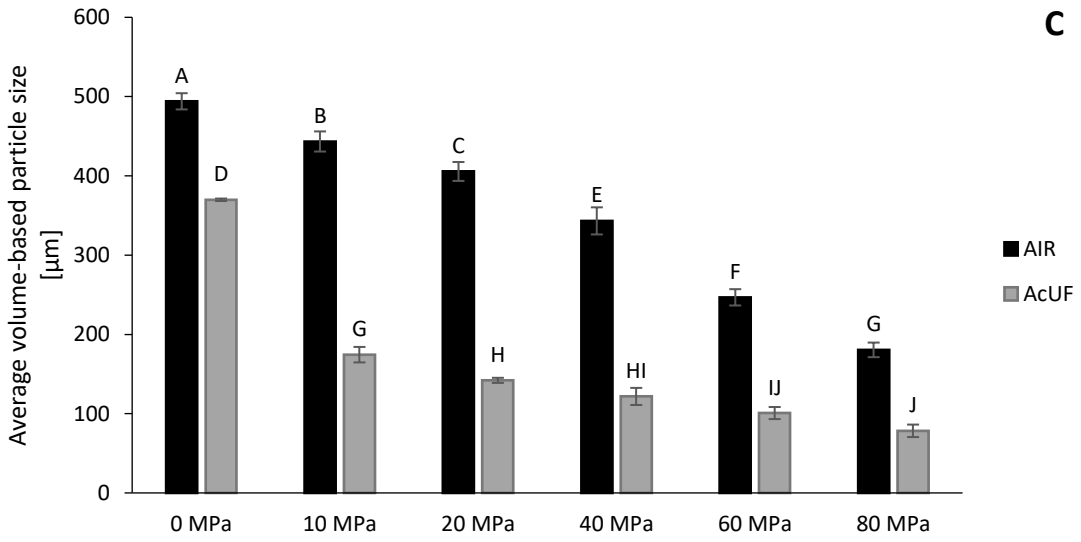

914

915 **Figure 2**: Volume-based particle size distribution of the suspensions prepared with the alcohol-insoluble
916 residue (AIR) (A) or the acid-unextractable fraction (AcUF) (B) and the average volume-based particle size
917 ($d_{4,3}$) of the AIR and AcUF suspensions (C) before (0 MPa) and after high-pressure homogenization
918 (performed at 1% w/w) at different pressure levels. The error bars represent the standard deviation
919 (n=2·2) and significant differences are indicated by different letters (Tukey test, $P < 0.05$).

920

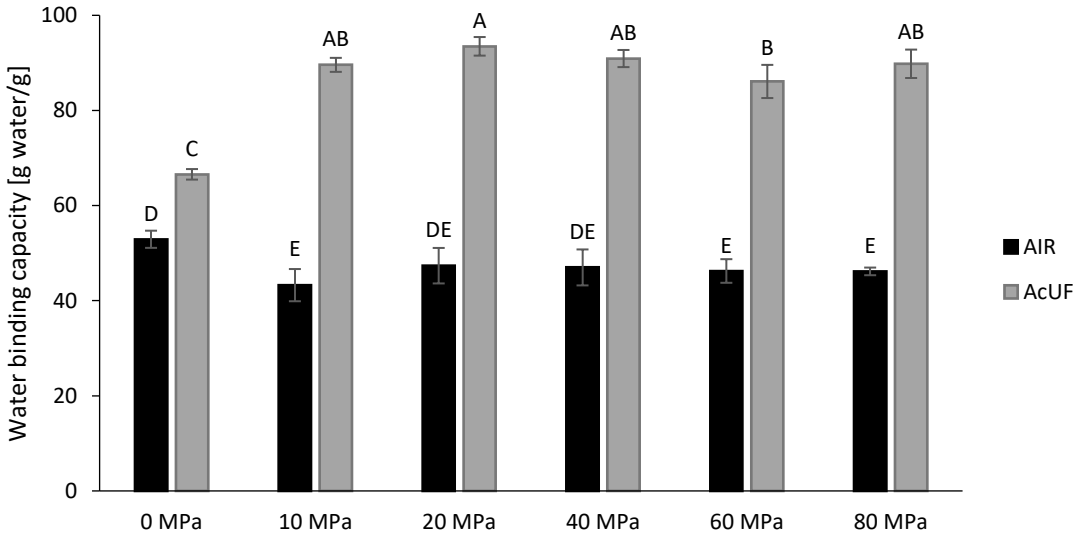

921

922 **Figure 3:** Water binding capacity at 1% (w/w) of the alcohol-insoluble residue (AIR) or acid-unextractable
923 fraction (AcUF) before (0 MPa) and after high-pressure homogenization at different pressure levels. The
924 error bars represent the standard deviation (n=2·2) and significant differences are indicated by different
925 letters (Tukey test, $P < 0.05$).

926

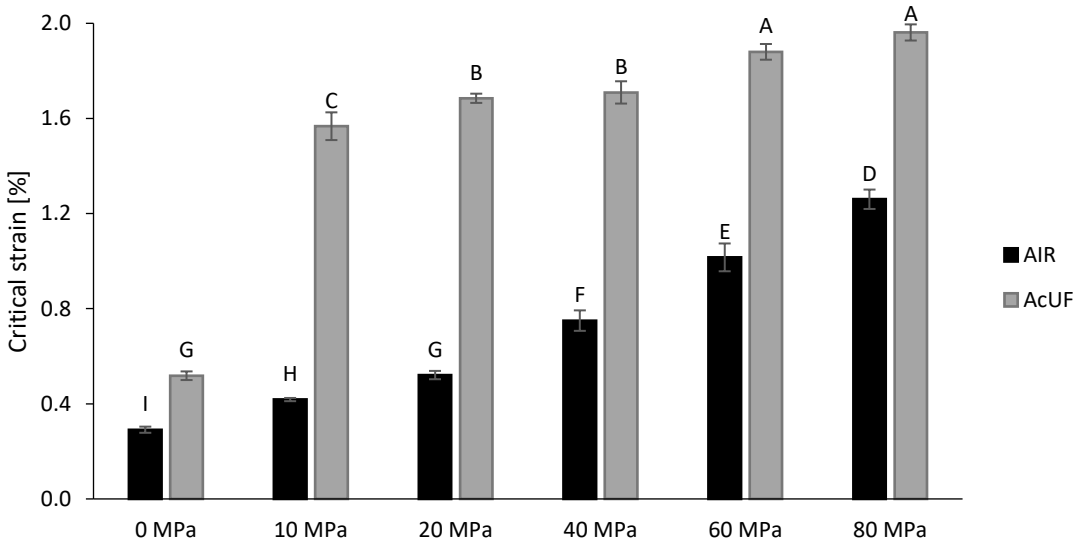

927

928 **Figure 4**: Critical strain of the suspensions (1% w/w) prepared with the alcohol-insoluble residue (AIR) or
929 acid-unextractable fraction (AcUF) before (0 MPa) and after high-pressure homogenization at different
930 pressure levels, obtained from the strain sweep at 10 rad/s angular frequency. The error bars represent
931 the standard deviation (n=2·2) and significant differences are indicated by different letters (Tukey test, P
932 < 0.05).

933

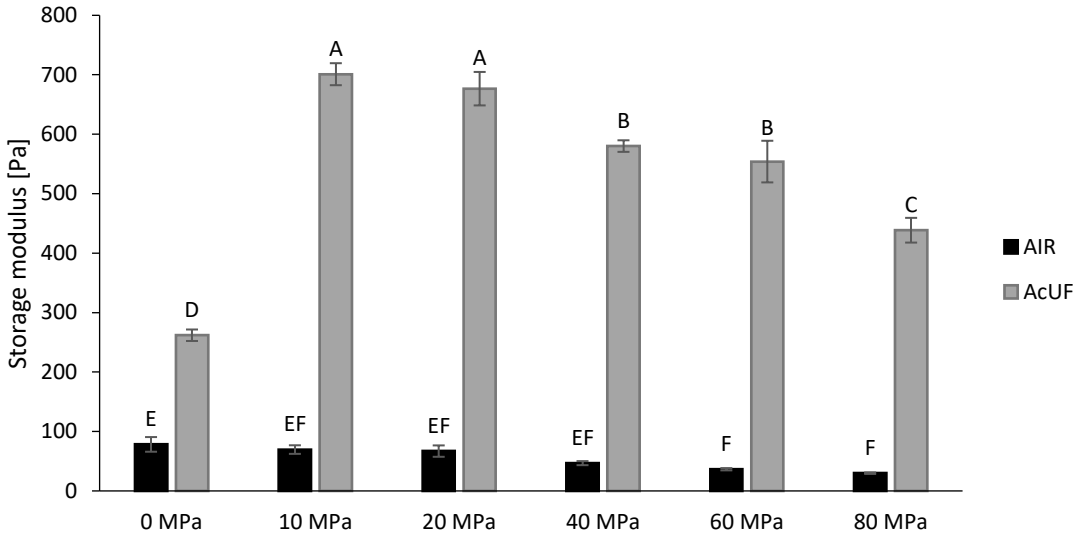

934

935 **Figure 5**: Storage modulus (G') of the suspensions (1% w/w) prepared with the alcohol-insoluble residue
936 (AIR) or unextractable fraction (UF) before (0 MPa) and after high-pressure homogenization at different
937 pressure levels, obtained from the frequency sweep at 10 rad/s angular frequency and 0.1% strain. The
938 error bars represent the standard deviation (n=2·2) and significant differences are indicated by different
939 letters (Tukey test, $P < 0.05$).

940

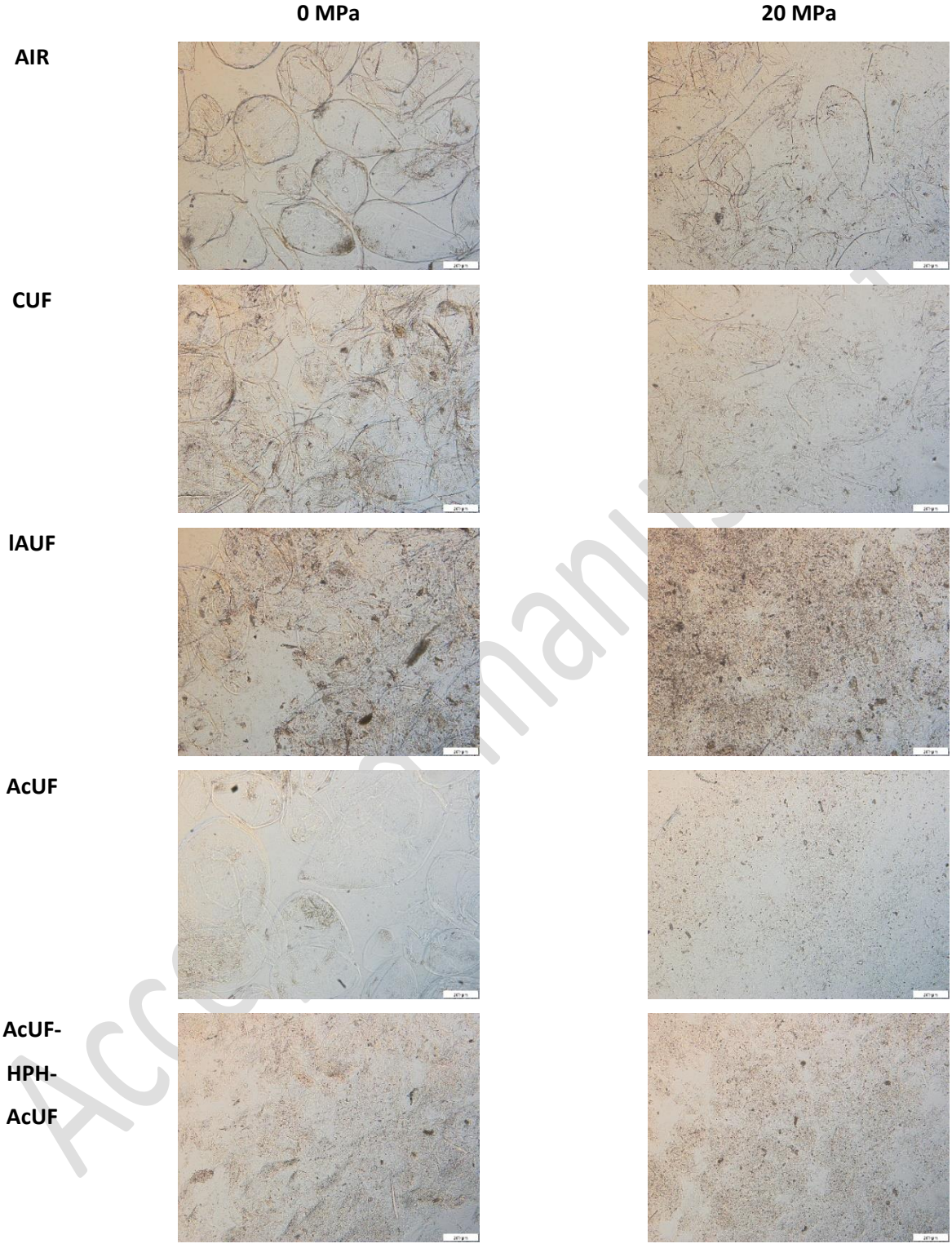

941

942

Figure 6: Microscopic visualization of the suspensions prepared with the alcohol-insoluble residue (AIR) or unextractable fraction (UF) at 0.6% (w/w) concentration before (0 MPa) and after high-pressure homogenization (20 MPa) (performed at 2% w/w). Scale bar represents 200 µm.

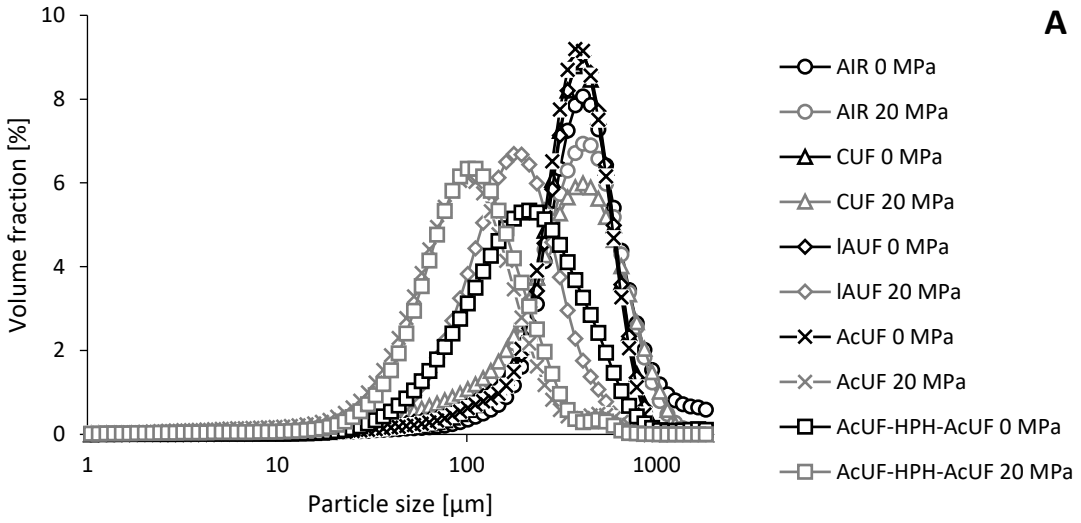

947

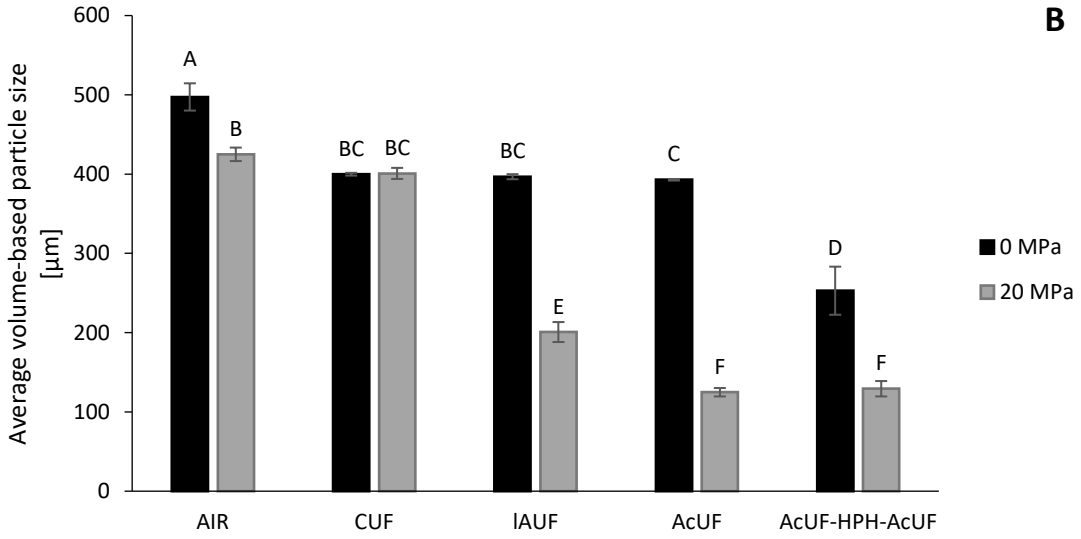

948

949 **Figure 7**: Volume-based particle size distribution (A) and average volume-based particle size ($d_{4,3}$) (B) of
950 the suspensions prepared with the alcohol-insoluble residue (AIR) or unextractable fraction (UF) before
951 (0 MPa) and after high-pressure homogenization (20 MPa) (performed at 2% w/w). The error bars
952 represent the standard deviation (n=2·2) and significant differences are indicated by different letters
953 (Tukey test, $P < 0.05$).

954

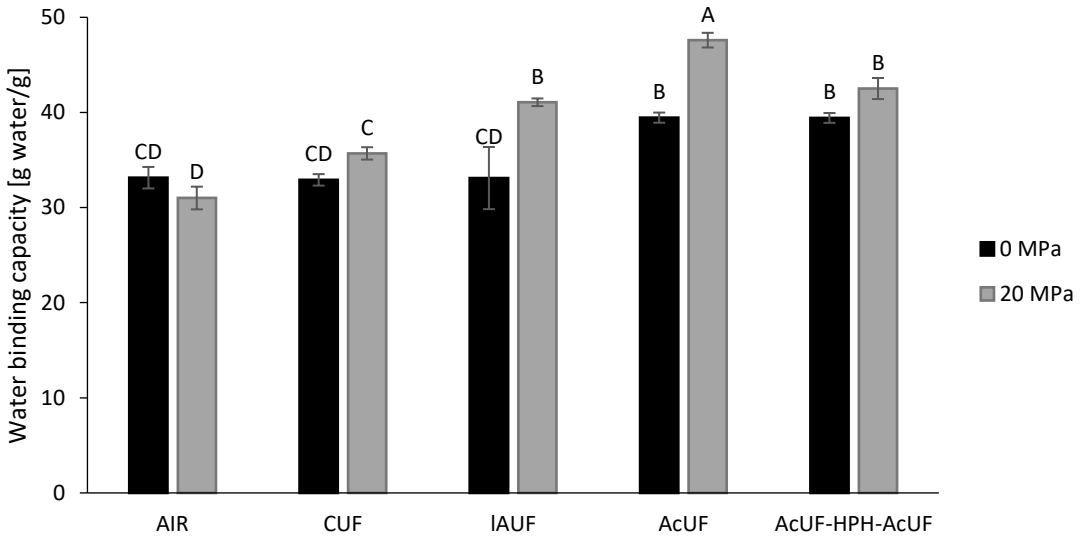

955

956 **Figure 8:** Water binding capacity at 2% (w/w) of the alcohol-insoluble residue (AIR) or unextractable
957 fraction (UF) before (0 MPa) and after high-pressure homogenization (20 MPa). The error bars represent
958 the standard deviation (n=2·2) and significant differences are indicated by different letters (Tukey test, P
959 < 0.05).

960

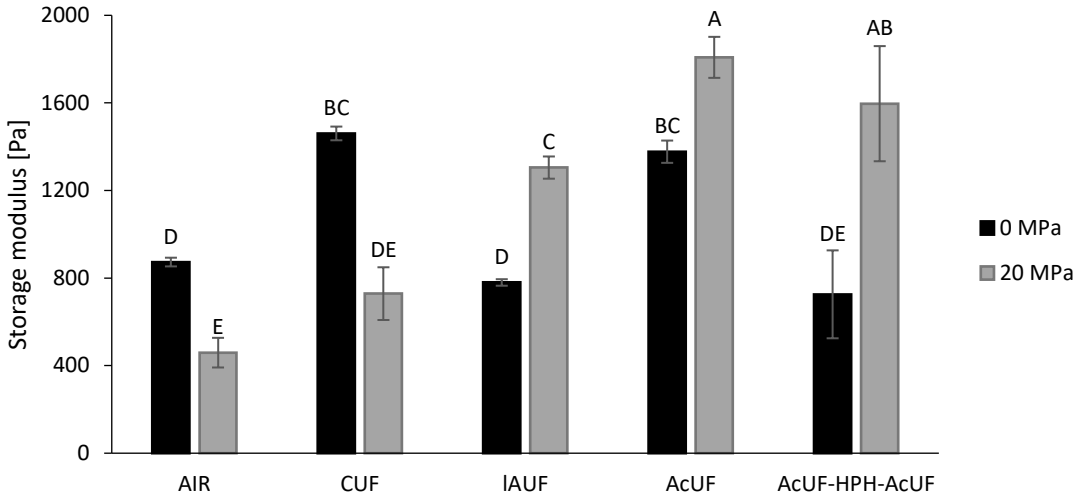

961

962 **Figure 9**: Storage modulus (G') of the suspensions (2% w/w) prepared with the alcohol-insoluble residue
963 (AIR) or unextractable fraction (UF) before (0 MPa) and after high-pressure homogenization (20 MPa),
964 obtained from the frequency sweep at 10 rad/s angular frequency and 0.1% strain. The error bars
965 represent the standard deviation (n=2·2) and significant differences are indicated by different letters
966 (Tukey test, $P < 0.05$).

967

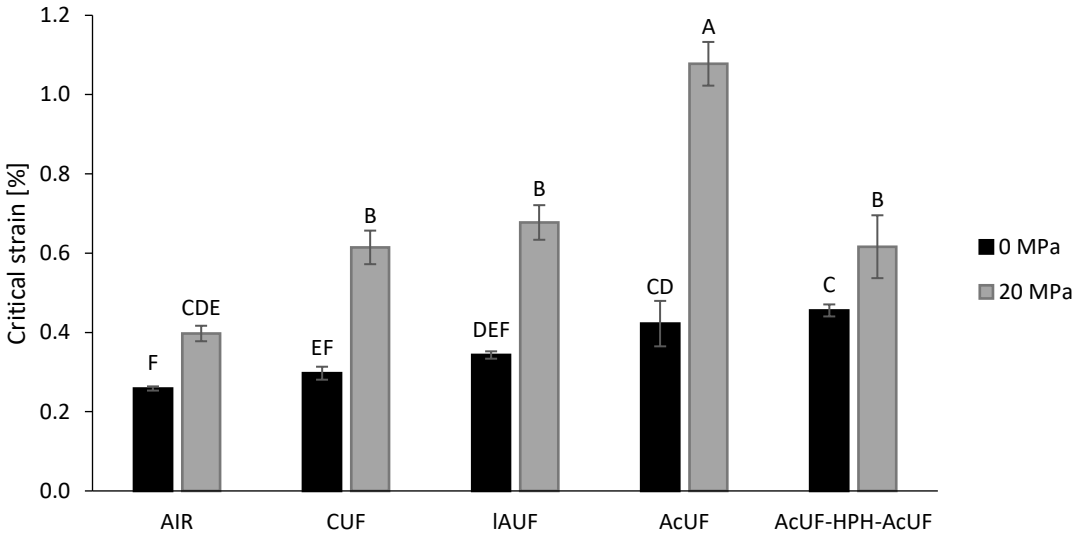

968

969 **Figure 10:** Critical strain of the suspensions (2% w/w) prepared with the alcohol-insoluble residue (AIR) or
970 unextractable fraction (UF) before (0 MPa) and after high-pressure homogenization (20 MPa), obtained
971 from the strain sweep at 10 rad/s angular frequency. The error bars represent the standard deviation
972 (n=2·2) and significant differences are indicated by different letters (Tukey test, $P < 0.05$).

973

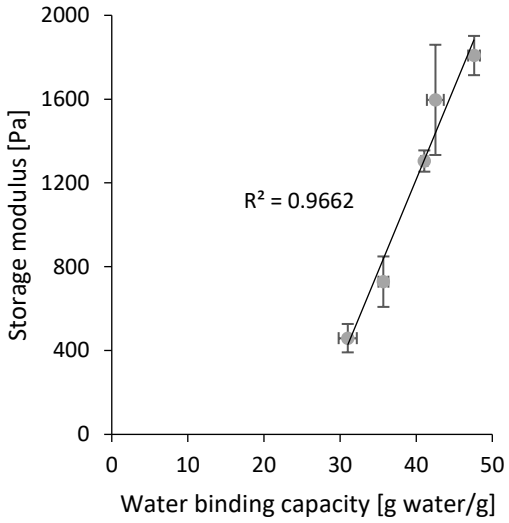

974

975 **Figure 11**: Relation between the storage modulus (G') of the CWM suspension (2% w/w) at 10 rad/s
976 angular frequency and 0.1% strain after high-pressure homogenization (20 MPa) and the water binding
977 capacity (WBC) of the respective CWM fraction at 2% (w/w). The error bars represent the standard
978 deviation (n=2·2).

979

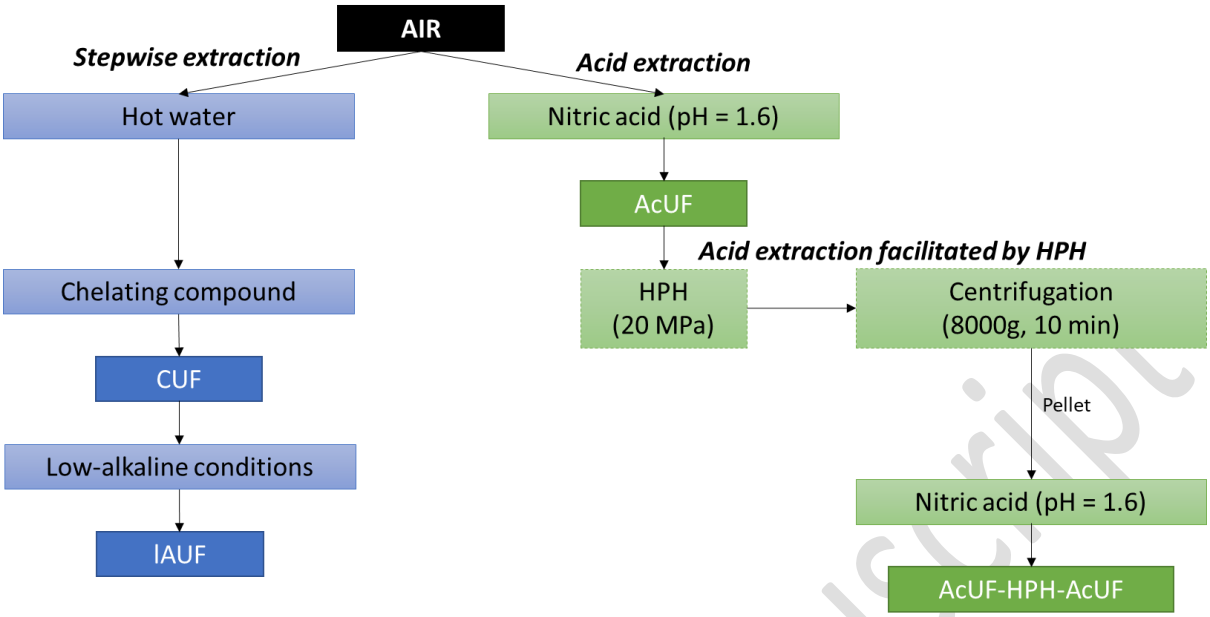

980

981 **Supplementary Figure 1:** Schematic overview of the chemical extractions performed to obtain the
982 different unextractable fractions. Figure is based on Van Audenhove, Bernaerts, De Smet, et al. (2021).

983 Van Audenhove, J., Bernaerts, T., De Smet, V., Delbaere, S., Van Loey, A. M., & Hendrickx, M. E. (2021).
984 The Structure and Composition of Extracted Pectin and Residual Cell Wall Material from Processing
985 Tomato: The Role of a Stepwise Approach versus High-Pressure Homogenization-Facilitated Acid
986 Extraction. *Foods*, *10*(5), 1064. https://doi.org/10.3390/foods10051064

987

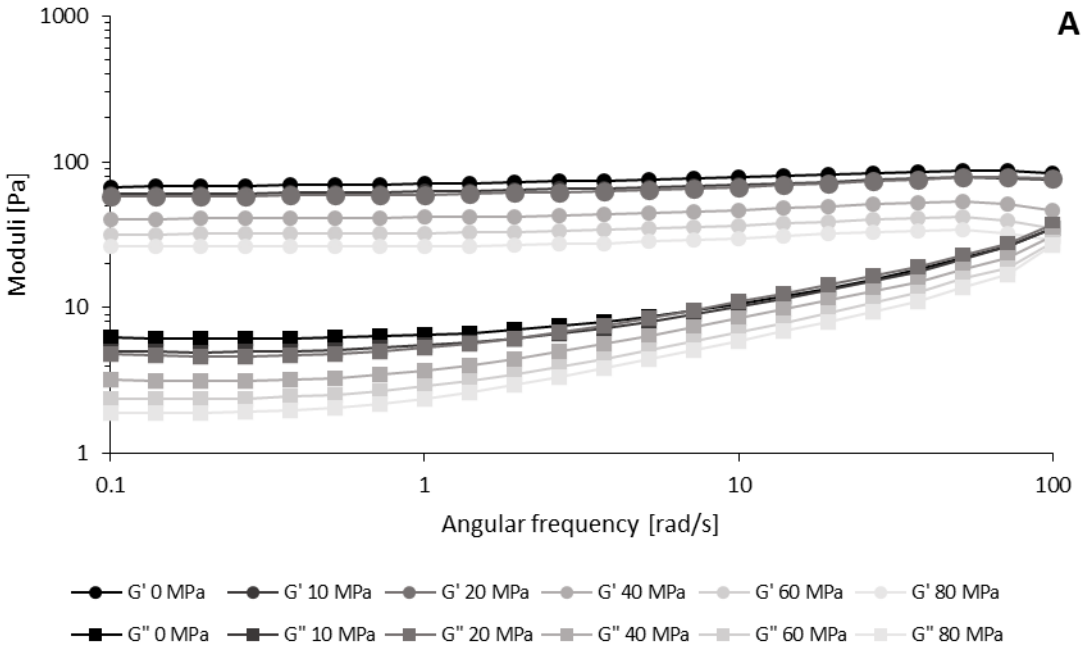

988

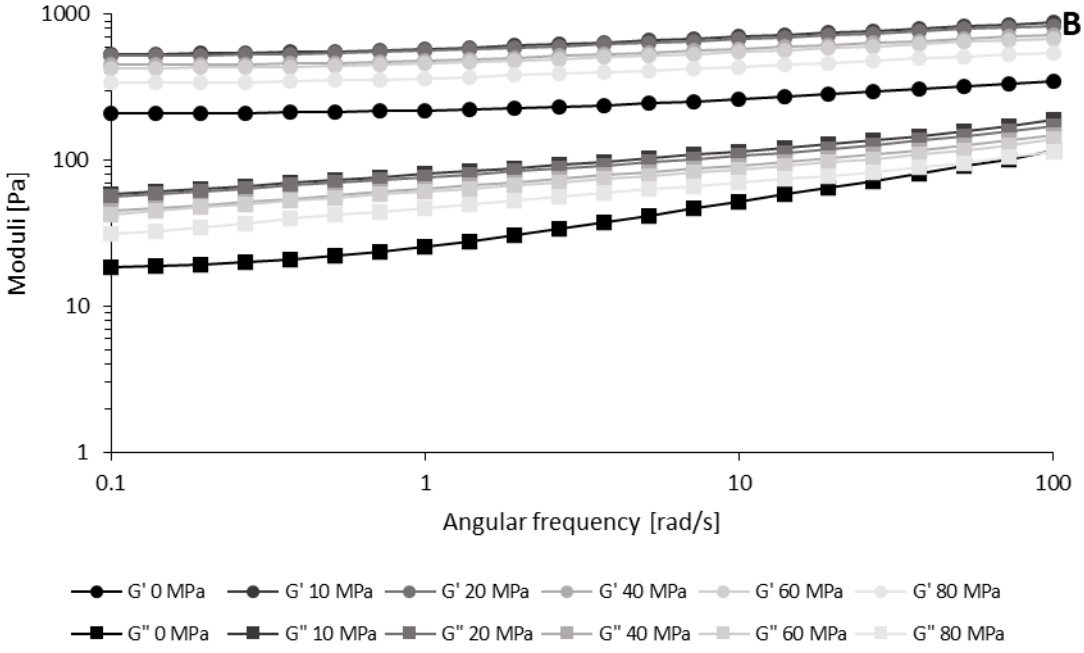

989

990 **Supplementary Figure 2**: Storage modulus (G') and loss modulus (G") in function of the angular frequency
991 (frequency sweep) at 0.1% strain of the suspension prepared with the alcohol-insoluble residue (AIR) (A)
992 or the acid-unextractable fraction (AcUF) (B) before (0 MPa) and after high-pressure homogenization at
993 different pressure levels.

994

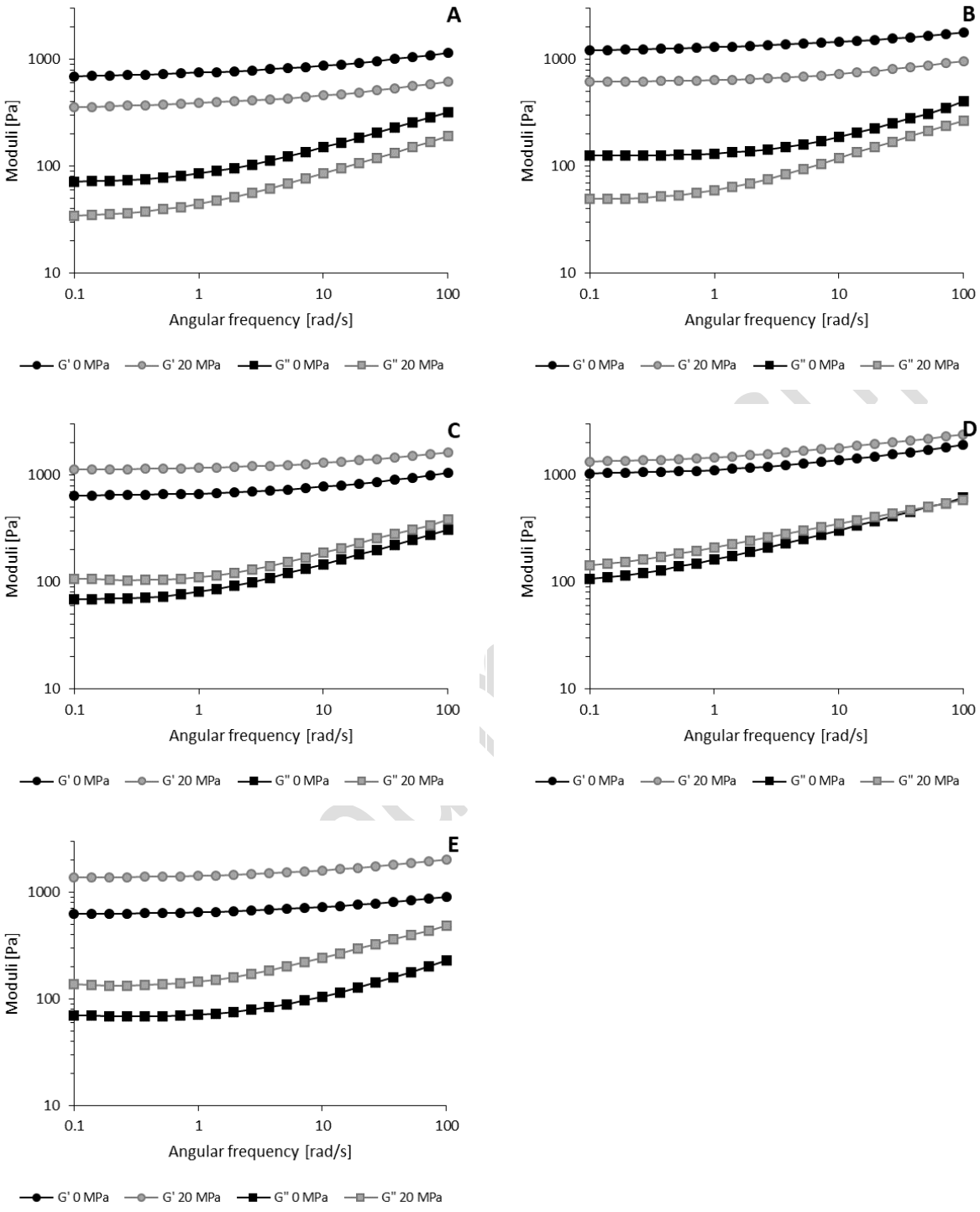

995 **Supplementary Figure 3**: Storage modulus (G') and loss modulus (G") in function of the angular frequency
996 (frequency sweep) at 0.1% strain of the suspensions prepared with the alcohol-insoluble residue (AIR) (A),
997 the chelator-unextractable fraction (CUF) (B), the low-alkaline-unextractable fraction (lAUF) (C), the acid-

unextractable fraction (AcUF) (D) and the acid-unextractable fraction of high-pressure homogenized AcUF (AcUF-HPH-AcUF) (E) before (0 MPa) and after high-pressure homogenization (20 MPa).